Cedar Lake, Wisconsin - Limnological response to alum treatment: 2024 interim report

Horse Creek at 10th Avenue

31 December 2024

University of Wisconsin – Stout
Center for Limnological Research and Rehabilitation
Department of Biology
260 Jarvis Hall
Menomonie, Wisconsin 54751
715-338-4395
jamesw@uwstout.edu

Executive Summary

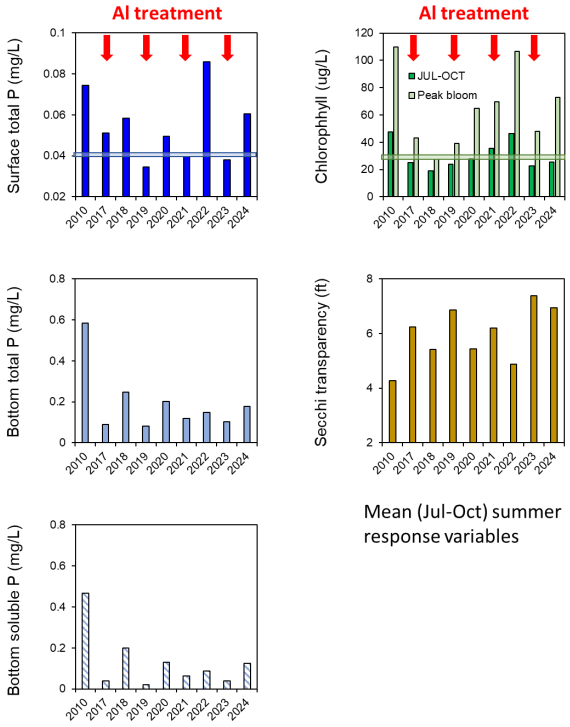

Mean (Jul-Oct) summer response variables

A comparison of mean summer (July-early October) summer concentrations of surface and bottom total phosphorus (P) and soluble reactive P (SRP), chlorophyll and Secchi transparency during a pretreatment year (2010) and the post-treatment years 2017-24.

- 2024 was a nontreatment year. The 4th partial alum application occurred in mid-July 2023. Approximately 26 g Al/m^2 were applied to depth contours between 20 and 25 ft and 17 g Al/m^2 were applied to depths > 25 ft. In addition, buffered alum was used for the 4th application to reduce sulfate input and loss of Fe (iron) in the lake.
- In 2024, the bottom waters became anoxic from late June through late August. Fall turnover and complete water column mixing resulted in reoxygenation by 5 September. Unfortunately, the 2023 alum treatment and Al floc layer at the sediment surface did not completely suppress internal P loading from sediments and soluble P diffused into the hypolimnion, attaining concentrations that ranged between 0.12 mg/L and 0.32 mg/L in August. Although not as high as pretreatment concentrations, this soluble P was mostly available for cyanobacteria uptake during Fall turnover, due to low dissolved iron relative to soluble P (i.e., Fe:P ratio).
- Chlorophyll concentrations increased after Fall turnover to > 60 µg/L in September. High winds in mid-September resulted in biomass pileup along shorelines.
- Although laboratory-derived sediment P flux has declined after 4 partial alum applications, rates still ranged between a mean 7.9 mg/m^2 d at depth > 25 ft and a mean 8.6 mg/m2 d within the 20-25-ft depth contour (i.e., alum treatment zones) as of 2024, which is unacceptably high. Pretreatment mean sediment P flux was ~ 18 mg/m^2 d. Lake P mass accumulation via internal P loading has also declined after 4 partial alum applications, but only by 42%.

- Poor WQ response outcomes in Cedar Lake are believed to be due to several factors. High rates of internal P loading are not being completely suppressed by the partial alum applications – i.e., the 17 to 50 g/m^2 partial doses applied biannually have become completely saturated with P and allow additional P to diffuse through the Al floc and into the bottom waters of the lake. Much higher Al doses on the order of > 40 g/m^2 over the > 20-ft depth contour may need to be applied over consecutive years (i.e., 2-4 years) to completely suppress internal P loading in the lake.
- Aluminum sulfate application has led to a reduction in redox-sensitive Fe. Cedar Lake has exhibited low Fe relative to P since pretreatment. Sulfate additions and apparent bacterial reduction to S in the sediment have led to FeS formation and irreversible loss of Fe from the iron cycle. Thus, there is now less Fe relative to P in the lake.
- The inability of partial biannual alum dose applications to completely control internal P loading coupled with leakage of P through the Al floc layer during the summer and low dissolved iron have led to worsening cyanobacterial blooms after Fall turnover, even after 4 partial alum applications.

- Addition of iron, as ferric chloride, to the lake may be a more cost-effective solution to controlling P availability to cyanobacteria than additional alum applications.

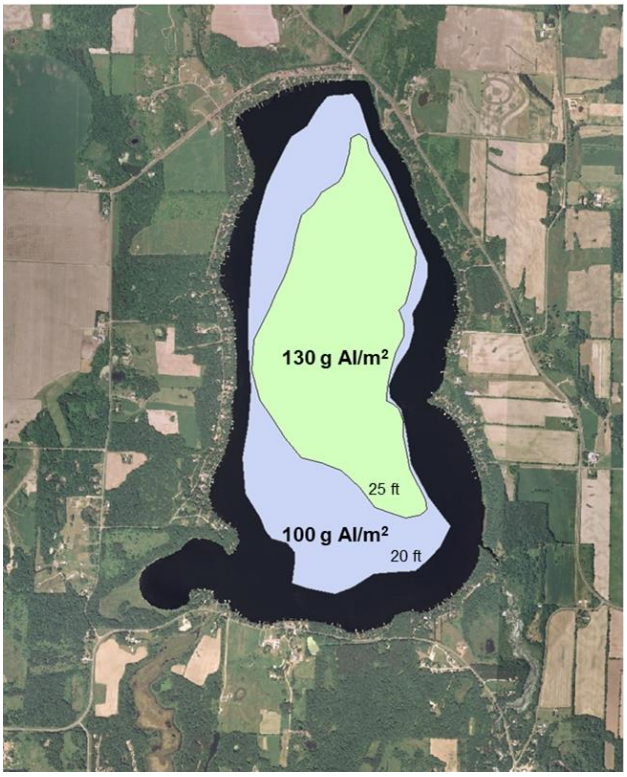

Alum dosage and application zones in Cedar Lake

Objectives

Multiple Al applications over a period of 10-12 years have been planned for Cedar Lake to control internal phosphorus loading. It is critical to conduct post-treatment monitoring of water and sediment chemistry to document

the trajectory of water quality improvement during rehabilitation to make informed decisions regarding adjusting management to meet future water quality goals. Post-treatment monitoring included field and laboratory research to document changes in 1) hydrology and watershed phosphorus (P) loading, 2) the P budget and lake water quality, 3) binding of sediment mobile P fractions that have contributed to internal P loading by alum, and 4) rates of diffusive P flux from the sediment under anaerobic conditions. Overall, lake water quality was predicted to respond to watershed and internal P loading reduction with lower surface concentrations of total P and chlorophyll concentrations throughout the summer, lower bloom frequency of nuisance chlorophyll levels, and higher water transparency. Multiple Al applications between 2017 and 2025 should result in the binding of iron-bound P and substantial reduction in diffusive P flux from sediments under anaerobic conditions (i.e., internal P loading).

Alum dose and application schedule for Cedar Lake Wisconsin.

Year	Chemical	Shallow Zone (20-25-ft)		Deep Zone (> 25 ft)	
		Discrete (g/m^2)	Cumulative (g/m^2)	Discrete (g/m^2)	Cumulative (g/m^2)
2017	Alum	20	20	26	26
2019	Alum	22	42	28.5	54.5
2021	Alum	0	42	50	104.5
2023	Buffered Alum	26	68	16.6	121.1
2025					
Subtotal		68		121.1	
Target		100		130	
Percent		68%		93%	
Deficit		32		8.9	

The first alum application occurred in late June 2017. The Al dose was 20 g/m^2 for sediment located within the 20-25 ft depth contour and 26 g/m^2 for sediment located at depths > 25 ft. The second alum application occurred during 11-22 June 2019 and Al concentrations ranged between 22 g/m^2 within the 20-25 ft depth contour and ~ 28 g/m^2 for depths > 25 ft. This combined Al application of 42 g/m^2 and 54 g/m^2 to the two depth zones ideally represented ~ 42% of the target Al doses of 100 g/m^2 and 130 g/m^2. However, sediment monitoring suggested the Al floc had spread and become diluted particularly at depths > 25 ft, resulting in lower measured Al concentrations than predicted. Lower Al recovery might be attributed to Al floc movement or redistribution and spread during and after application by wind activity and water currents. Al floc movement during settling is not uncommon and has been reported to occur in other alum treatments (Egemose et al. 2009, 2013; Huser 2017; James and Bischoff 2020). As an adaptive management decision, the third alum treatment in June 2021 was applied to sediments located at depths > 25 ft only to increase the overall Al concentration and thickness of the Al floc in this deeper area of the lake. Since this area is smaller than the earlier combined application area

encompassing depths > 20 ft (332 ac), the Al dosage was increased to ~ 50 g/m^2 within the > 25-ft zone without increasing overall costs.

The fourth alum application occurred in 2023. It was hypothesized that use of aluminum sulfate for the first 3 treatments led to interference with the iron cycle in the lake via iron sulfide formation as a result of bacterial reduction of sulfate to S by anaerobic bacteria at the sediment-water interface. Because P binding in the Al floc layer was still not complete due to partial dosage application, some sediment P has still been diffusing through the Al floc layer into the water column. P availability during fall turnover in 2022 led to a cyanobacteria bloom with chlorophyll concentrations exceeding 100 μg/L.

In 2023, application strategy was changed 4-fold to improve P binding efficiency. First, the product was switched to buffered alum to reduce sulfate input to the lake. Second, since no alum was applied to the 20-25-ft depth contour in 2021, a higher alum dose was applied to the 20-25-ft depth contour in 2023 to achieve dosage requirements in this area of the lake. Third, to meet budget constraints (since buffered alum is more expensive than aluminum sulfate), the buffered alum dose was reduced to 26 g Al/m^2 applied to the 20-25-ft depth contour and 16.6 g Al/m^2 applied to the > 25-ft depth contour. Finally, the alum application window was moved to mid-July, just before anticipated turnover, to strip any hypolimnetic P from the water column to minimize P uptake by cyanobacteria.

The objectives of this interim report are to describe the 2024 limnological and sediment variable response to these alum treatments in Cedar Lake. Limnological monitoring is being used in conjunction with an adaptive management approach to gauge lake response and the need, if any, to adjust Al dose or application strategy.

Methods

Watershed loading and lake monitoring

A gauging station was established on Horse Creek above Cedar Lake at 10th Ave for

concentration, loading, and flow determination between May and October 2024 (Fig. 1). Unfortunately, the flow velocity equipment was vandalized and destroyed in late July 2021. A water level pressure transducer (Onset, Inc) was deployed and maintained by Polk County soil and Water Conservation District in 2024. US-Stout CLRR also placed a backup monitor at that location. Discrete flow velocity measurements were collected at biweekly intervals between May and October 2024 using a Marsh-McBirney Flow-Mate 2000 velocity probe to develop a stage elevation-flow relationship for estimating continuous flow from the continuous stage elevation record. Grab samples were collected biweekly at the 10th Ave gauging station for chemical analysis. Water samples were analyzed for total P and soluble reactive P (SRP) using standard methods (APHA 2011). Summer tributary P loading was calculated using the computer program FLUX.

The deep basin water quality station WQ 2 was sampled biweekly between May and October 2024 (Fig. 1). An integrated sample over the upper 2-m was collected for analysis of total P, SRP, and chlorophyll a. Additional discrete samples were collected at 1-m intervals to within 0.5 m of the sediment surface for analysis of total P, SRP, and chlorophyll. Bottom samples were also analyzed for total and dissolved iron. These samples were analyzed by the University of Wisconsin Water and Environmental Analysis Laboratory using inductively-coupled plasma atomic absorption spectroscopy. Secchi transparency and in situ measurements (temperature, dissolved oxygen, pH, and conductivity) were collected on each date using a YSI 6600 sonde (Yellow Springs Instruments) that was calibrated against dissolved oxygen Winkler titrations (APHA 2011) and known buffer solutions.

Sediment chemistry

Sediment characteristics. A sediment core was collected in August 2024 at WQ 2 (Fig. 1) for determination of vertical profiles of various sediment characteristics and phosphorus fractions (see Analytical methods below). The sediment core was sectioned at 1-cm intervals between 0 and 10 cm and at 2-cm intervals below the 10-cm depth for determination of moisture content, wet and dry bulk density, loss-on-ignition organic matter, loosely-bound P, iron-bound P, labile organic P, aluminum-bound P, and total aluminum. Additional cores were collected at stations 2,

3, 8, 10, 18,20, and 24 (Fig. 1). An upper 10 cm slice was sectioned for the variables listed above.

Laboratory-derived diffusive phosphorus flux from sediments under anaerobic conditions. Anaerobic diffusive P fluxes were measured from intact sediment cores collected at stations shown in Figure 1 in August 2024. Three sediment cores were collected at WQ 2 and one sediment core was collected at each spatial station to monitor alum treatment effectiveness after 2024 alum application. The sediment incubation systems were placed in a darkened environmental chamber and incubated at 20 C for up to 7 days. The incubation temperature was set to a standard temperature for all stations for comparative purposes. The oxidation-reduction environment in each system was controlled by gently bubbling nitrogen through an air stone placed just above the sediment surface to maintain anaerobic conditions.

Water samples for SRP were collected from the center of each system using an acid-washed syringe and filtered through a 0.45 µm membrane syringe filter (Nalge). The water volume removed from each system during sampling was replaced by addition of filtered lake water preadjusted to the proper oxidation-reduction condition. These volumes were accurately measured for determination of dilution effects. Rates of P release from the sediment (mg/m^2 d) were calculated as the linear change in mass in the overlying water divided by time (days) and the area (m^2) of the incubation core liner. Regression analysis was used to estimate rates over the linear portion of the data.

Analytical methods. A known volume of sediment was dried at 105 ^oC for determination of moisture content, wet and dry bulk density, and burned at 550 ^oC for determination of loss-on-ignition organic matter content (Avnimelech et al. 2001, Håkanson and Jansson 2002). Phosphorus fractionation was conducted according to Hieltjes and Lijklema (1980), Psenner and Puckso (1988), and Nürnberg (1988) for the determination of ammonium-chloride-extractable P (loosely-bound P), bicarbonate-dithionite-extractable P (i.e., iron-bound P), and sodium hydroxide-extractable P (i.e., aluminum-bound P).

The loosely-bound and iron-bound P fractions are readily mobilized at the sediment-water

interface as a result of anaerobic conditions that lead to desorption of P from sediment and diffusion into the overlying water column (Mortimer 1971, Boström 1984, Nürnberg 1988). The sum of the loosely-bound and iron-bound P fraction represents redox-sensitive P (i.e., the P fraction that is active in P release under anaerobic and reducing conditions) and will be referred to as ***redox-P***. Aluminum-bound P reflects P bound to the Al floc after aluminum sulfate application and its chemical transformation to aluminum hydroxide ($Al(OH)_3$).

Summary of Results

Hydrology and phosphorus loading

On an annual basis, precipitation in 2024 was near the~ 33-inch average since 1980 at ~33 inches (Fig. 2). Monthly precipitation at Amery in 2024 was above the long-term average in May, June, and August, and below average in July and September (Fig. 3). Storms producing 2 inches of rain occurred in late May, and mid- and late August (Fig. 4). Storms exceeding 1 inch occurred in early June. Flow at Horse Creek (10th Ave) exhibited numerous peaks in May and June in response to storms (Fig. 4). Flow subsided in July then increased in early August in conjunction with the 2-inch rainfall recorded at Amery WI. Flow declined again during draughty conditions in September. Summer mean daily flow at 10th Ave in 2024 was relatively high at 0.90 m^3/s compared to other years (Fig. 5).

Table 1. Mean summer (May-October) constituent concentrations and loading for the Horse Creek inflow station at 10th Ave. Summer loading could not be determined in 2023 due to logger failures during the summer.

Year	Variable	TSS	Total P	SRP
2010	Concentration (mg/L)		0.089	0.031
	Load (kg/d)		4.18	1.42
2017	Concentration (mg/L)	15.2	0.084	0.034
	Load (kg/d)	767.8	4.26	1.71
2018	Concentration (mg/L)	16.5	0.100	0.039
	Load (kg/d)	549	3.36	1.28
2019	Concentration (mg/L)	10.6	0.083	0.035
	Load (kg/d)	524	4.07	1.72
2020	Concentration (mg/L)		0.083	0.033
	Load (kg/d)		6.14	2.35
2021	Concentration (mg/L)[1]	22.1	0.082	0.021
	Load (kg/d)[2]	945	3.49	0.88
2022	Concentration (mg/L)	13.9	0.070	0.023
	Load (kg/d)	584	2.93	0.97
2023	Concentration (mg/L)	8.65	0.066	0.021
	Load (kg/d)	Not determined - Logger failure		
2024	Concentration (mg/L)		0.066	0.027
	Load (kg/d)		5.26	2.16

Flow logger vandalized

[1]Represents a flow-weighted mean between APR-JUL only

[2]Represents an estimated daily load between APR-JUL only

Total P concentrations in Horse Creek at 10th Ave were highest in May 2024, ranging between 0.095 mg/L and 0.105 mg/L (Fig. 6). Although soluble reactive P was relatively low in May, concentrations increased to a peak of 0.037 mg/L in late July. Total P (0.097 mg/L) and soluble reactive P concentrations (0.058 mg/L) increased to another maximum in early August during a storm-related inflow period. Late

August-early September P concentration increases were associated with a peak in the hydrograph that occurred during the same period.

Concentration-flow relationships in 2024 generally fell within historical patterns (Fig. 7). Flow-averaged summer total P in 2024 was 0.066 mg/L, comparable to other years (Table 1 and Fig. 7). The flow-averaged SRP concentration was 0.027 mg/L and accounted for ~ 41% of the total P in 2024. Summer total and soluble P loading was higher in 2024 compared to recent years, coinciding with greater precipitation and flow.

Lake limnological response

Stratification developed in mid-June and persisted until late August (Fig. 8). Hypolimnetic anoxia also developed in conjunction with stratification in mid-June and persisted until the late August turnover. Bottom anoxia was usually confined depths ≥ 7 m. The lake completely mixed in lake August, resulting in reoxygenation of the entire water column. Temporary stratification developed in mid-September but the hypolimnion remained oxygenated. Complete water column mixing and oxygenated conditions occurred again in early October.

Unfortunately, bottom P concentrations increased steadily in 2024 after the establishment of hypolimnetic anoxia (Fig. 9). Concentrations exceeded 0.31 mg/L total P and 0.28 mg/L soluble P by the end of August. Late August turnover resulted in mixing of both total and soluble P throughout the water column (Fig. 10). In particular, soluble P exceeded 0.04 mg/L throughout the water column in September and August. This P was available for cyanobacterial uptake and coincided with a bloom in early September (Fig. 10).

Surface total P concentrations were relatively low (≤ 0.020 mg/L) between May and the end of August (Fig. 10 and 11). However, concentrations increased after the late August turnover period and coincided with the development of an algal bloom between mid-September and October, suggesting uptake of P for cyanobacteria growth.

Chlorophyll concentrations were very low between May and late August, averaging only 11 µg/L

(Fig. 10 and 12, Appendix I). Fall turnover in late August and mixing of hypolimnetic soluble P throughout the water column coincided with a severe bloom in early September (Fig. 10 and 12, Appendix I). Concentrations exceeded 60 µg/L of 5 and 17 September. High winds in late September pushed cyanobacteria biomass to the shoreline areas and open water concentrations declined to < 20 µg/L in October. Overall, total P and chlorophyll were significantly related, indicating P limitation of algal growth (Fig. 14).

Secchi transparency exceeded 3 m (10 ft) between late May and late July 2024 (Fig. 13). It declined to 1.6 m to 1.9 m in August. Minima in Secchi transparency to 1.3 m (4.3 ft) occurred in conjunction with Fall turnover and the early September cyanobacteria bloom. Secchi transparency deepened in late October to 3.2 m (10.5 ft) as the bloom subsided. Secchi transparency generally exhibited a significant inverse pattern to that of chlorophyll in 2024, indicating that light extinction was due to algae versus inorganic turbidity (Fig. 14).

A comparison of mean summer (July-early October) limnological response variables before alum treatment (i.e., 2010) versus 2024 is shown in Figure 15 and Table 2. Mean bottom total P and SRP concentrations increased during the nontreatment year 2024 as a result of internal P loading and flux through the Al floc layer (Fig. 15). As mentioned above, this internal P load was directly available for cyanobacteria uptake during the Fall turnover period. Mean summer surface total P increased to 0.061 mg/L in 2024 compared to the treatment year 2023. Mean July-early October chlorophyll was 25.6 µg/L in 2024. However, the WisCALM (2024) 15 July-30 September mean was 35 µg/L, which exceeded the mean 27 µg/L goal for the lake. Finally, mean Secchi transparency was 6.9 ft (Fig. 15 and Table 2).

Table 2. Summary of changes in lake water quality and sediment variables after the initial alum treatment in June 2017. Overall goals after completion of the treatment schedule are shown in the last column.

Variable			2010	2017	2018	2019	2020	2021	2022	2023	2024	Percent improvement over 2010 means								Goal after internal P loading
												2017	2018	2019	2020	2021	2022	2023	2024	
Lake	Mean (Jul-Oct)	Mean surface TP (mg/L)	0.074	0.051	0.058	0.035	0.050	0.040	0.086	0.038	0.061	31% reduction	22% reduction	53% reduction	34% reduction	47% reduction	15% increase	49% reduction	19% reduction	< 0.040
		Mean bottom TP (mg/L)	0.583	0.088	0.246	0.082	0.203	0.120	0.148	0.102	0.178	85% reduction	58% reduction	86% reduction	65% reduction	79% reduction	75% reduction	83% reduction	70% reduction	< 0.050
		Mean bottom SRP (mg/L)	0.467	0.038	0.199	0.02	0.130	0.062	0.086	0.038	0.125	92% reduction	57% reduction	96% reduction	72% reduction	87% reduction	82% reduction	92% reduction	73% reduction	< 0.050
		Mean chlorophyll (ug/L)	47.63	25.17	19.08	24.31	27.88	35.66	46.31	22.57	25.57	47% reduction	60% reduction	49% reduction	41% reduction	25% reduction	3% reduction	53% reduction	46% reduction	< 15
		Mean Secchi transparency (ft)	4.27	6.28	5.41	6.81	5.43	6.19	4.88	7.38	6.93	46% increase	27% increase	59% increase	27% increase	45% increase	14% increase	73% increase	62% increase	12.1
	Early Fall peak (i.e. late August-early October)	Surface TP (mg/L)	0.130	0.081	0.115	0.042	0.074	0.060	0.136	0.061	0.130	38% reduction	11% reduction	68% reduction	43% reduction	54% reduction	5% increase	53% reduction	0% reduction	NA
		Bottom TP (mg/L)	1.216	0.13	0.543	0.206	0.510	0.223	0.227	0.210	0.318	89% reduction	55% reduction	83% reduction	58% reduction	82% reduction	81% reduction	83% reduction	74% reduction	NA
		Bottom SRP (mg/L)	1.092	0.068	0.468	0.092	0.442	0.156	0.193	0.085	0.289	94% reduction	57% reduction	92% redcution	60% redcution	86% reduction	82% reduction	92% reduction	74% reduction	NA
		Chlorophyll (ug/L)	109.6	42.95	27.63	42.00	64.89	69.70	106.50	48.02	73.00	61% reduction	75% reduction	62% reduction	41% reduction	36% reduction	3% reduction	56% reduction	33% reduction	NA
		Secchi transparency (ft)	2.66	3.61	3.63	3.94	3.12	3.61	2.63	3.60	1.30	36% increase	37% increase	48% increase	17% increase	36% increase	1% reduction	35% increase	51% increase	NA
Sediment[1]		Net internal P loading (kg/d)	3,723	1,150	2,123	-177	1,351	404	3,103	955	2,522	69% reduction	42% reduction	100% reduction	64% reduction	89% reduction	17% reduction	74% reduction	32% reduction	< 400
		Net internal P loading (mg/m^2 d)	8.8	3.2	5.6	-0.5	2.8	1.1	8.5	3.9	5.2	64% reduction	36% reduction	100% reduction	68% reduction	88% reduction	3% reduction	56% reduction	41% reduction	< 1.5
		Sediment diffusive P flux (mg/m^2 d)	15.01	11.83	8.34	1.26	4.66	3.72	3.68	6.5	9.9	21% reduction	29% reduction	85% reduction	69% reduction	75% reduction	75% reduction	57% reduction	40% reduction	< 1.5
		Redox-P (mg/g)	0.457	0.298	0.307	0.238	0.415	0.295	0.317	0.355	0.305	35% reduction	33% reduction	48% reduction	9% reduction	36% reduction	30% reduction	22% reduction	33% reduction	< 0.100
		Al-bound P (mg/g)	0.097	0.170	0.331	0.216	0.342	0.308	0.225	0.248	0.229	75% increase	241% increase	123% increase	253% increase	218% increase	132% increase	157% increase	136% increase	NA

[1]Stations 2, 8, 13, 18, and 24

Lakewide P mass accumulation was more pronounced in 2024 compared to alum application years (Fig. 16 and 17). P mass in the lake increased in conjunction with the buildup of hypolimnetic P starting in July and continued through the Fall turnover period. The lake-wide net internal P load during this 111-day period was 23 kg/d, which was higher than the 2023 alum application year (Table 3). When normalized with lake surface area, the P mass accumulation rate rebounded (i.e., increased) to 5.1 mg/m^2 d 2024 (Fig. 18).

Table 3. Summer net internal phosphorus loading ($P_{net\ int\ load}$) estimates (bold font) for Cedar Lake in 2010 (pretreatment) and 2017-24 (post-treatment).

Summer	Period	$P_{tributary}$	$P_{discharge}$	$P_{retention}$	$P_{lake\ storage}$	$P_{net\ int\ load}$		
	(d)	(kg)	(kg)	(kg)	(kg)	(kg)	(kg/d)	(mg/m^2 d)
2010	97	445	238	207	3,931	**3,723**	**38**	**8.8**
2017	83	349	212	137	1,287	**1,150**	**14**	**3.2**
2018	87	292	128	164	2,288	**2,123**	**24**	**2.8**
2019	85	346	141	205	28	**-77**	**-1**	**0**
2020	112	456	369	87	1,434	**1,351**	**12**	**2.8**
2021[1]	84	293	84	210	614	**404**	**5**	**1.1**
2022	84	246	283	-37	3,066	**3,103**	**37**	**8.5**
	56[2]	164	68	96	923	**827**	**15**	**3.4**
	42[3]	123	175	-52	2,092	**2,144**	**51**	**11.7**
2023	56	164	33	131	1,086	**955**	**17**	**3.9**
2024	111	588	465	124	2,646	**2,522**	**23**	**5.2**

[1] $P_{tributary}$, $P_{discharge}$, and $P_{retention}$ are estimates for the period May through July only due to flow logger vandalism.

[2]Only for the period 5/23/22 to 7/18/22 - i.e., before the mid-summer turnover

[3]Only for the period 7/18/22 to 8/29/22 - i.e., after the mid-summer turnover

[4]Estimated from the summer 2022 due to logger failure in 2023

One of the concerns over aluminum sulfate application is removal of Fe from recycling as a result of treatment. Cedar Lake hypolimnetic total and dissolved Fe were low relative to SRP before treatment (James et al. 2015). The hypolimnetic total Fe:P ratio was only ~ 1.4:1 mass, indicating insufficient Fe to bind all of the hypolimnetic P during fall turnover and chemical oxidation of Fe to Fe(OOH). Thus, some of the soluble P was directly available for algal uptake and bloom formation during turnover.

Addition of aluminum sulfate can indirectly reduce hypolimnetic Fe by its reaction with S to form FeS, which is inert and becomes buried from further recycling. The sulfate byproduct of alum application is reduced by anaerobic bacteria in the profundal sediment to form S, which then reacts with Fe to form insoluble FeS.

Bottom iron patterns in Cedar Lake in 2024 continued to suggest that concentrations have declined from pretreatment values in 2010 (Fig. 19). Mean Jun-Aug bottom concentrations have remained lower by~ 50% in 2024 compared to 2010 (Table 4a). Approximately one week before Fall turnover in 2024, total and dissolved iron were low relative to total and soluble P, resulting in a low Fe:P ratio in the bottom waters (Fig. 20 and Table 4b). Thus, the Fe concentration was insufficient to bind all the soluble P during turnover, resulting in P availability for cyanobacteria uptake and growth. The ideal Fe:P ratio minimum to bind all soluble P is 3.6:1 mass and 2:1 molar. In 2023, the alum application reduced soluble P concentrations in the bottom waters to the point that the Fe:P ratio approached the minimum threshold (Fig. 20). The fall cyanobacteria bloom was more modest in 2023 as a result. Ideally, an Fe:P ratio of > 5:1 mass would ensure complete scavenging of soluble P during Fall overturn.

Table 4a. Mean (late June - end of August) summer bottom iron concentrations in Cedar Lake in 2010 (before Al) and in 2023 and 2024 (after 4 Al applications).

JUN-AUG	Total Fe	Dissolved Fe	Total P	SRP	Total Fe:P		Dissolved Fe:P	
	(mg/L)	(mg/L)	(mg/L	(mg/L)	(mass)	(molar)	(mass)	(molar)
					(3.6)	(2.0)	(3.6)	(2.0)
2010	1.18	0.59	0.836	0.702	1.58	1.28	0.81	0.45
2023	0.53	0.28	0.101	0.038	5.56	3.08	8.55	4.74
2024	0.45	0.31	0.199	0.147	2.34	1.30	2.87	1.59

Table 4b. Bottom iron concentrations in Cedar Lake during Fall turnover in 2010 (before Al) and 2023 and 2024 (after 4 Al applications).

Turnover	Total Fe	Dissolved Fe	Total P	SRP	Total Fe:P		Dissolved Fe:P	
	(mg/L)	(mg/L)	(mg/L	(mg/L)	(mass)	(molar)	(mass)	(molar)
					(3.6)	(2.0)	(3.6)	(2.0)
2010 (8/24/10)	1.45	0.40	0.823	0.762	1.77	1.06	0.52	0.29
2023 (8/22/23)	0.53	0.14	0.134	0.049	4.65	2.58	4.09	2.27
2024 (8/21/24)	0.29	0.37	0.318	0.289	0.90	0.50	1.27	0.71

Changes in sediment chemistry and anaerobic diffusive phosphorus flux

Laboratory-derived anaerobic P flux from sediment collected at the WQ station rebounded during the nontreatment year 2024 and was high at 11.4 mg/m^2 d s (Fig. 21). While anaerobic P flux was still lower compared to pretreatment fluxes (representing a 36% reduction), rates need to be much lower and on the order of < 1.5 mg/m^2 d in order to meet WQ targets. Spatially, anaerobic P fluxes ranged between 4.2 mg/m^2 d and 11.4 mg/m^2 d at depths > 25 ft (25% to 71% reduction) and between 5.8 mg/m^2 d and 12.1 mg/m^2 d within the 20-25-ft depth contour (1% to 56% reduction, Fig. 22). Mean anaerobic P fluxes were similar in the 2 alum treatment zones (mean 7.9 mg/m^2 d at depths > 25 ft and 8.6 mg/m2 d at the 20-25-ft depth zone), representing a 53% reduction at depths > 25 ft and a 30% reduction for the 20-25-ft depth contour (Fig. 23).

Sediment profiles at the WQ station indicated that added alum was located in the upper 8 cm in the sediment core collected at the WQ station located roughly in the center of the lake at a depth > 25 ft in 2024 (Fig. 24). Below 8 cm, Al concentrations declined to baseline at this station. The area-based Al concentration in the upper 8-cm at the WQ station was ~ 81 g/m^2, close to the theoretical ~ 120 g/m^2 applied to depths > 25 ft since 2017. Along the N-S transect running down the approximate center of the lake, mean Al concentrations in the upper 8 cm sediment layer were similar stations located at depths > 25 ft versus those located between the 20 and 25-ft depth contour (Fig. 25). To date, ~ 68 g Al/m^2 have been applied to the 20-25-ft depth contour.

Spatial variations in redox-P and aluminum-bound P in the upper 10-cm sediment layer are shown in Fig. 26 for stations located in the recently alum-treated zone (i.e., depths > 25 ft) and the 20-ft to 25-ft depth zone. Overall, redox-P concentrations have generally declined (negative percent or reduction) as a result of binding onto the Al floc layer while aluminum-bound P concentrations have generally increased (positive percent or increase), reflecting P bound to alum. Notable exceptions in redox-P changes included 2 stations in the > 25-ft depth contour and 3 stations located in the SW region of the 20-25-ft depth contour (Fig. 26). Increases in aluminum-bound P have been greatest for sediments located at depths > 25 ft (Fig. 23 and 26). These patterns coincided with a greater mean aluminum-bound P concentration in the upper 10-cm sediment layer within the > 25-ft depth contour versus the mean within the 20-25-ft depth

contour (Fig. 23).

At station WQ 2, vertical variations in sediment chemistry indicated continued binding of P onto the Al floc (Fig. 27). Aluminum-bound P concentrations were elevated in the upper 9-cm layer as of August 2024, compared to pretreatment concentrations. In contrast, concentrations of redox-P (i.e., sediment P that contributes to internal P loading) have declined in the surface sediment compared to the pretreatment concentration peaks (Fig. 27). However, concentrations are still elevated near the sediment surface and can contribute to internal P loading to the lake.

Conclusions and Recommendations

It is apparent that after 4 partial alum applications to Cedar Lake, internal P loading is still a significant source of P that drives cyanobacteria blooms and high chlorophyll during periods of Fall turnover and mixing of largely available soluble P throughout the water column. Although soluble P concentrations have decreased in the hypolimnion during the summer and internal P loading has decreased by 30 to 50%, sediment P flux is still unacceptably high at ~ 8 mg/m^2 d. Poor lake WQ response and improvement suggests that the partial alum doses ranging between 16.6 g/m^2 and 50 g/m^2 spread out biannually have not been high enough to completely suppress internal P loading. Much higher alum doses (> 40 g/m^2 over the 20-ft depth contour at a minimum) applied over consecutive years (3 consecutive years minimum) would be needed. In addition, dissolved iron concentrations have become further depleted in the hypolimnion with aluminum sulfate additions. While dissolved Fe was low relative to P before the start of management, additional concentration declines may have coincided with bacterial sulfate reduction at the sediment-water interface and formation of iron sulfide (FeS), a solid that irreversibly buries Fe from any further recycling. Inability of the partial alum treatments to control internal P loading, leakage of P through the Al floc layer, permanent loss of Fe as FeS, and a further decline in the hypolimnetic Fe:P ratio have led to worsening cyanobacteria blooms with high chlorophyll after Fall turnover.

Two possible management options are available for consideration. First, additional high alum dose treatments could be applied over consecutive years to control internal P loading. This

option would be the most expensive. A second option would be to add enough iron to supplement to current applied Al floc layer. The goal of iron application, added initially as ferric chloride, is to bind soluble P that has leaked through the Al floc layer and mixed into the water column during Fall turnover. Added iron would become reduced by anaerobic bacteria during summer anoxia and diffuse into the bottom waters as dissolved reduced Fe^{2+}. At a 5:1 Fe:P mass ratio, dissolved reduced Fe^{2+} becomes chemically oxidized during turnover and reaeration to a precipitate $Fe(OH)_3$, binds with soluble P, and settles back to the sediment. $Fe(OOH)\sim PO_4$ is difficult to assimilate for cyanobacteria growth. Supplementing the lake with iron would be less expensive.

References

APHA (American Public Health Association). 2011. Standard Methods for the Examination of Water and Wastewater. 22th ed. American Public Health Association, American Water Works Association, Water Environment Federation.

Avnimelech Y, Ritvo G, Meijer LE, Kochba M. 2001. Water content, organic carbon and dry bulk density in flooded sediments. Aquacult Eng 25:25-33.

Boström B. 1984. Potential mobility of phosphorus in different types of lake sediments. Int. Revue. Ges. Hydrobiol. 69:457-474.

de Vicente I, Huang P, Andersen FØ, Jensen HS. 2008. Phosphate adsorption by fresh and aged aluminum hydroxide. Consequences for lake restoration. Environ Sci Technol 42:6650-6655.

Egemose SG, Wauer G, Kleeberg A. 2009. Resuspension behavior of aluminum treated lake sediments: effects of aging and pH. Hydrobiologia 636: 203-217.

Egemose SG, Reitzel K, Andersen FØ, Jensen HS. 2013. Resuspension-mediated aluminum and phosphorus distribution in lake sediments after aluminum treatment. Hydrobiologia 701: 79-88.

Håkanson L, Jansson M. 2002. Principles of lake sedimentology. The Blackburn Press, Caldwell, NJ USA.

Hjieltjes AH, Lijklema L. 1980. Fractionation of inorganic phosphorus in calcareous sediments. J Environ Qual 8: 130-132.

Hondzo M, Feyaerts T, Donovan R, O'Connor BL. 2005. Universal scaling of dissolved oxygen distribution at the sediment-water interface: A power law. Limnol Oceanogr 50:1667-1676.

Huser BJ. 2017. Aluminum application to restore water quality in eutrophic lakes: maximizing binding efficiency between aluminum and phosphorus. Lake Reserv Manage 33: 143-151.

James WF. 2012. Limnological and aquatic macrophyte biomass characteristics in Half Moon Lake, Eau Claire, Wisconsin, 2012: Interim letter report. University of Wisconsin – Stout, Sustainability Sciences Institute – Discovery Center, Menomonie, WI.

James WF. 2014. Phosphorus budget and management strategies for Cedar Lake, WI. University of Wisconsin – Stout, Sustainability Sciences Institute – Discovery Center, Menomonie, WI.

James WF. 2017. Phosphorus binding dynamics in the aluminum floc layer of Half Moon Lake, Wisconsin. Lake Reserv Manage 33:130-142.

James WF, Bischoff JM. 2020. Sediment aluminum:phosphorus binding ratios and internal phosphorus loading characteristics 12 years after aluminum sulfate application to Lake McCarrons, Minnesota. Lake Reserv Manage 36:1-13.

James WF, PW Sorge, PJ Garrison. 2015. Managing internal phosphorus loading in a weakly stratified eutrophic lake. Lake Reserv Manage 31:292-305.

Mortimer CH. 1971. Chemical exchanges between sediments and water in the Great Lakes – Speculations on probable regulatory mechanisms. Limnol Oceanogr 16:387-404.

Nürnberg GK. 1988. Prediction of phosphorus release rates from total and reductant-soluble phosphorus in anoxic lake sediments. Can J Fish Aquat Sci 45:453-462.

Nürnberg GK. 2009. Assessing internal phosphorus load – Problems to be solved. Lake Reserv Manage 25:419-432.

Pilgrim KM, Huser BJ, Brezonik PL. 2007. A method for comparative evaluation of whole-lake and inflow alum treatment. Wat Res. 41:1215-1224.

Psenner R, Puckso R. 1988. Phosphorus fractionation: Advantages and limits of the method for the study of sediment P origins and interactions. Arch Hydrobiol Biel Erg Limnol 30:43-59.

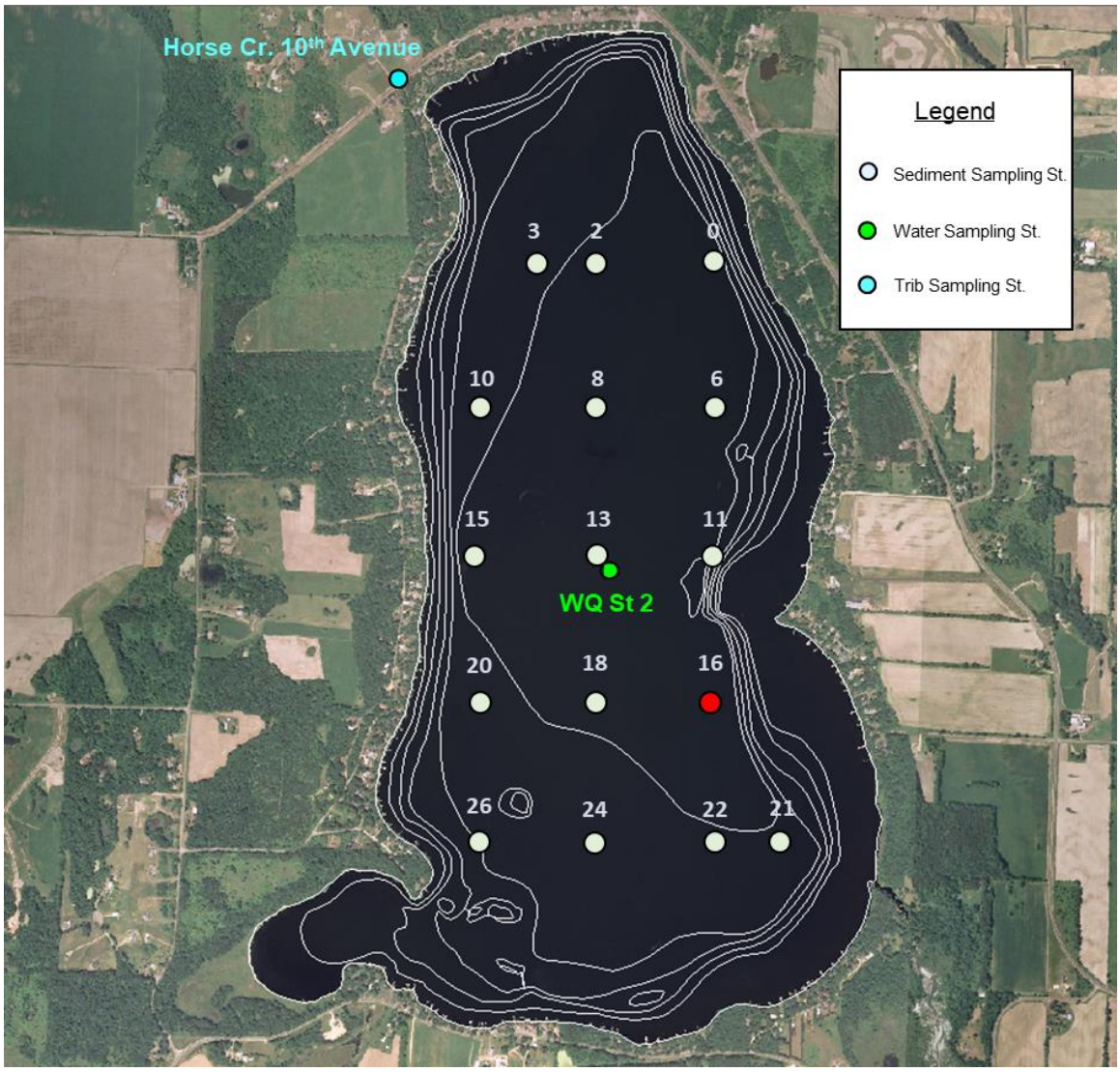

Figure 1. Sediment and water sampling stations in 2024. There was not enough sediment for analysis from the cores collected at Station 16.

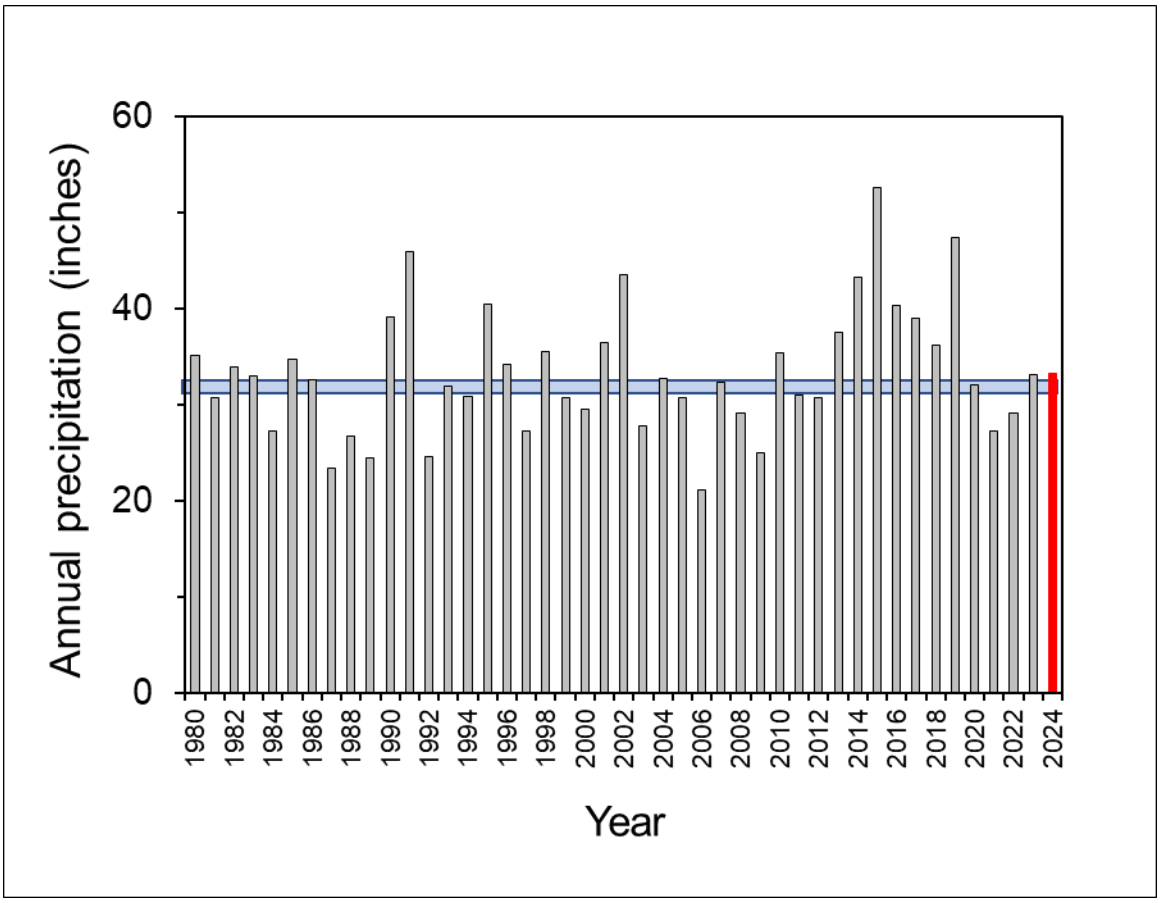

Figure 2. Variations in annual precipitation at Amery, WI. Blue horizontal line represents the average. The year 2024 is highlighted in red.

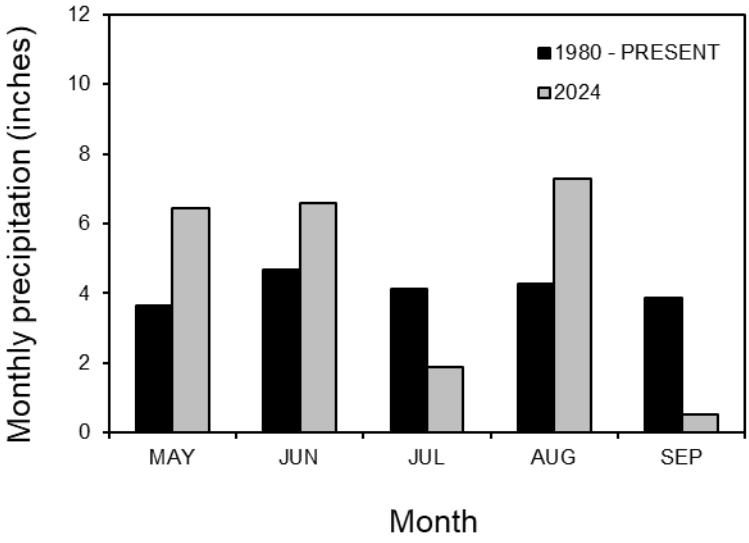

Figure 3. A comparison of average monthly precipitation.

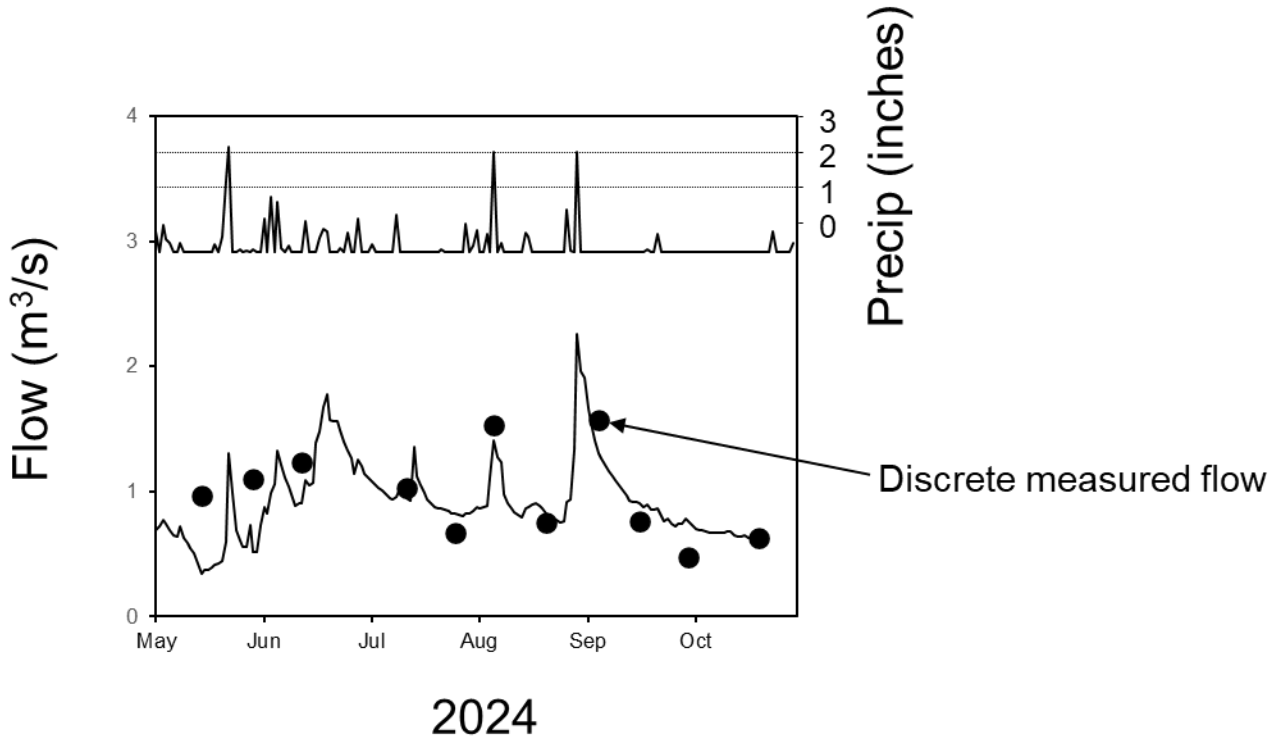

Figure 4. Seasonal variations in daily precipitation at Amery, WI, and flow for Horse Creek at 10th Ave.

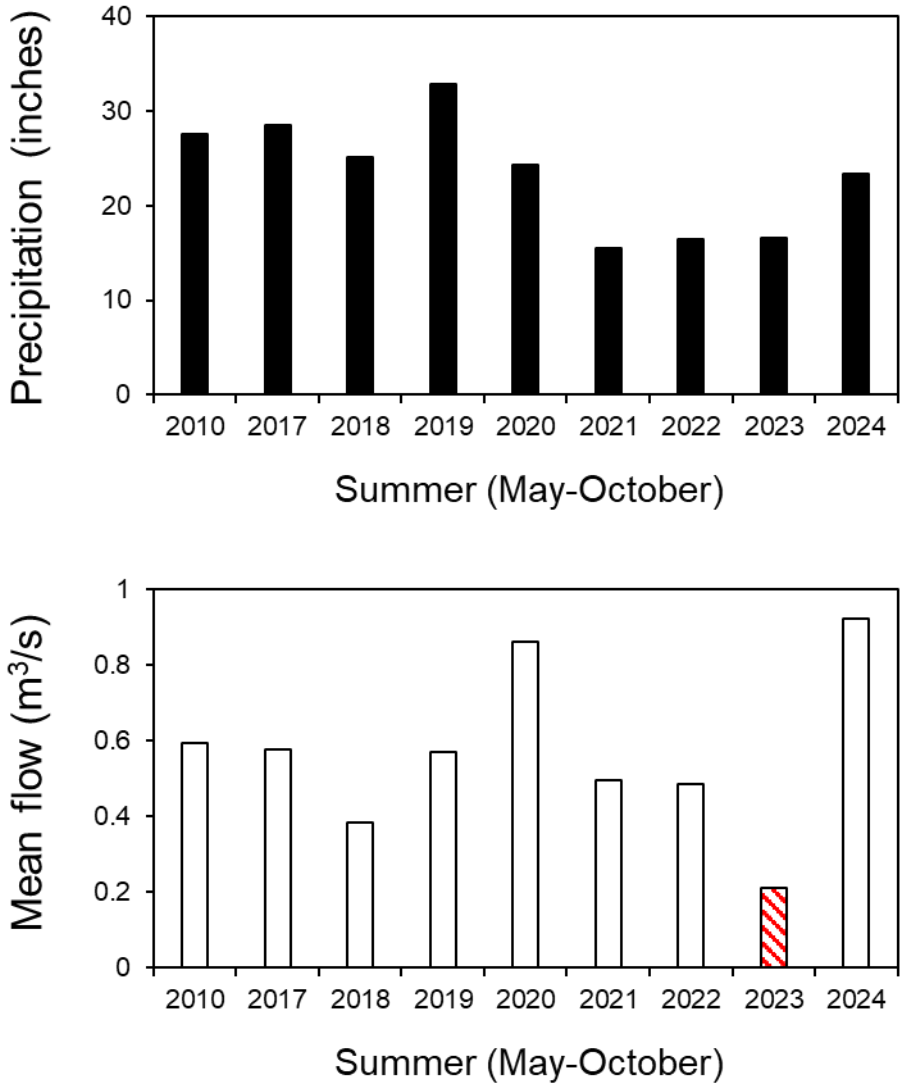

Figure 5. A comparison of summer (May-October) precipitation (upper panel) and mean Horse Creek flow (lower panel). The summer of 2010 was a pretreatment year. Alum was applied to the lake in late June 2017, 2019, 2021, and 2023. The mean flow for 2023 is probably an underestimate due to logger failure.

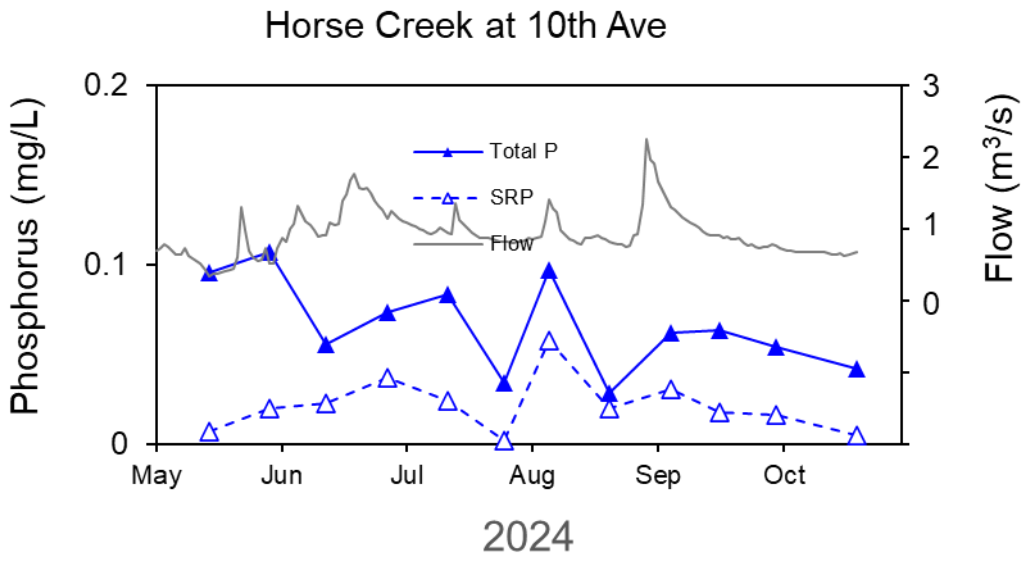

Figure 6. Seasonal variations in total phosphorus (P) and soluble reactive P (SRP) concentration at Horse Creek 10th Ave (i.e., mouth to Cedar Lake).

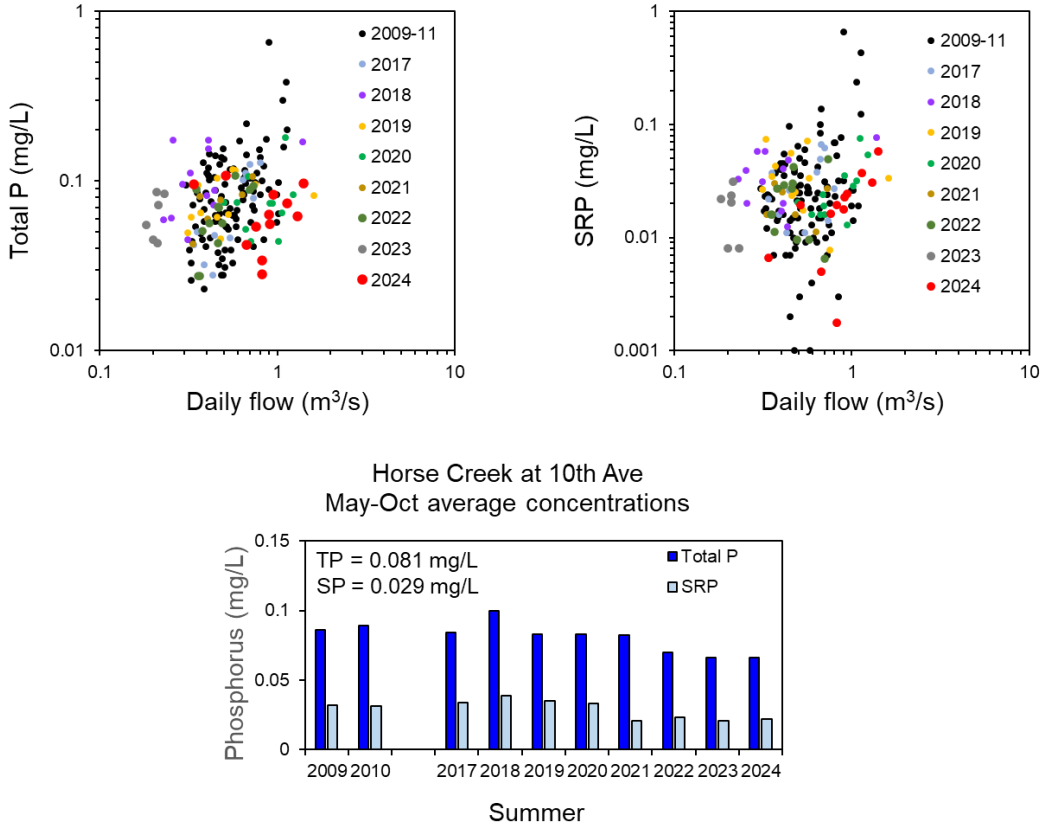

Figure 7. Phosphorus (P) concentration versus daily flow at Horse Creek at 10th Ave. Flows may be underestimated for 2023 due to logger failure.

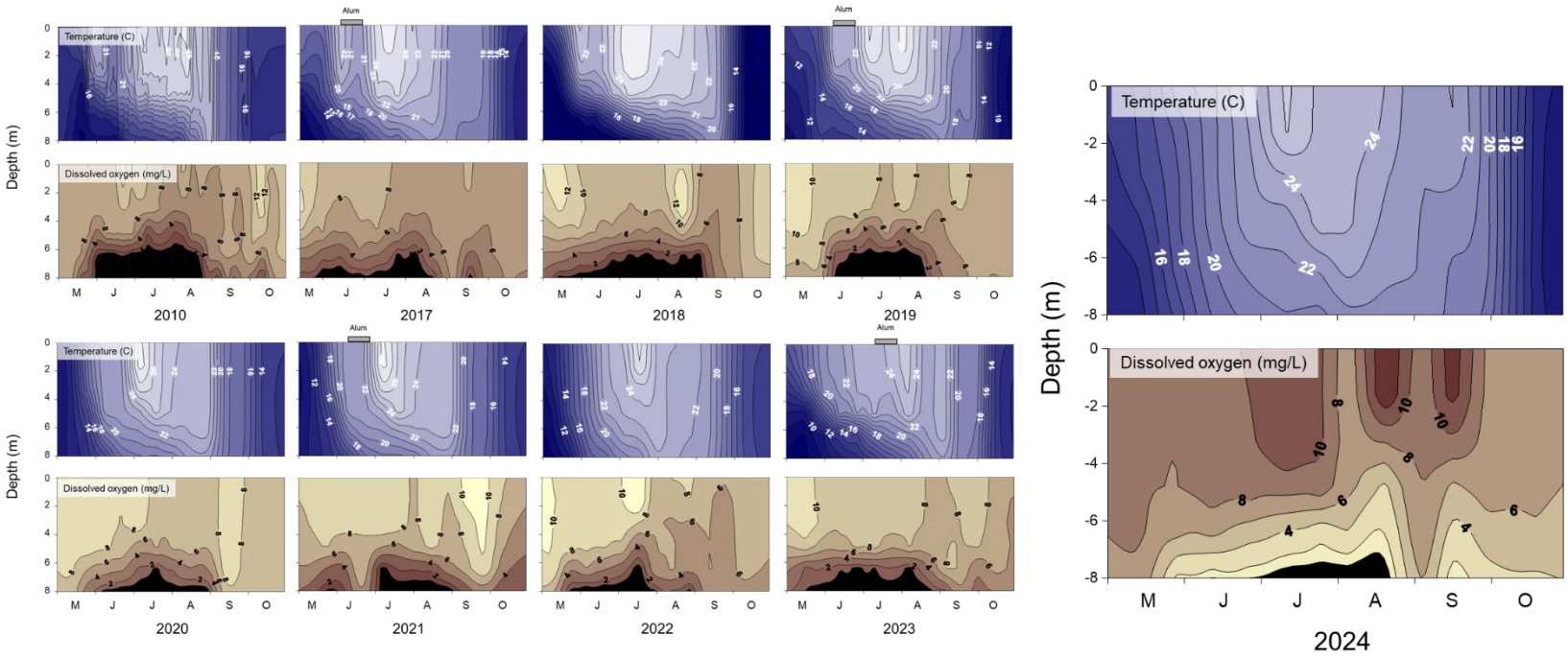

Figure 8. Seasonal and vertical variations in temperature (upper panels) and dissolved oxygen (lower panels) in 2010 (pre-treatment) and 2017-2024 (after alum treatment). Alum was applied in June 2017, 2019, 2021, and 2023.

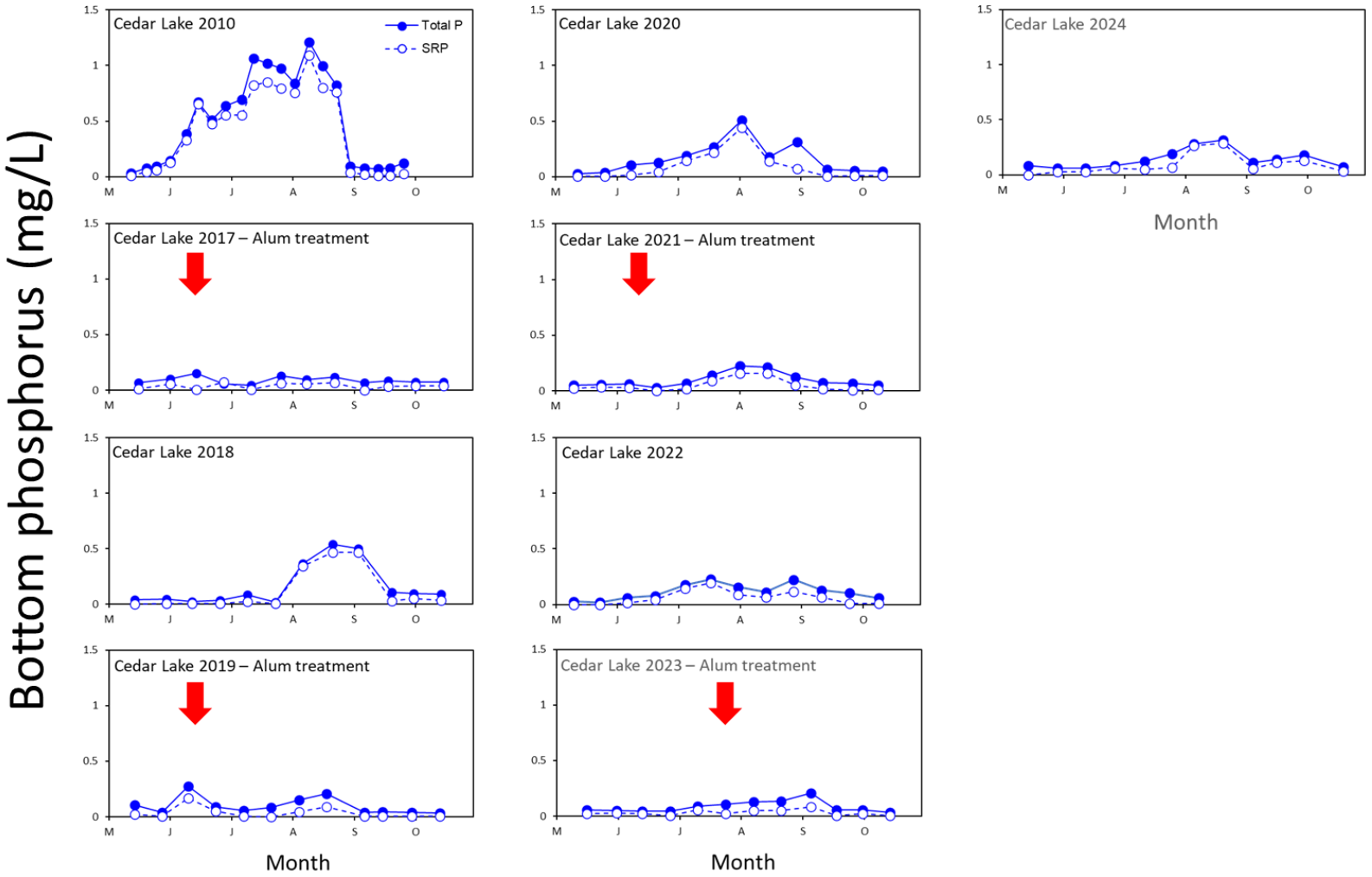

Figure 9. Seasonal variations in bottom (i.e., ~ 0.25 m above the sediment-water interface) total phosphorus (P), and bottom soluble reactive P (SRP) during a pretreatment year (2010) and the post-alum treatment years 2017-24. Alum was applied in June 2017, 2019, 2021, and 2023.

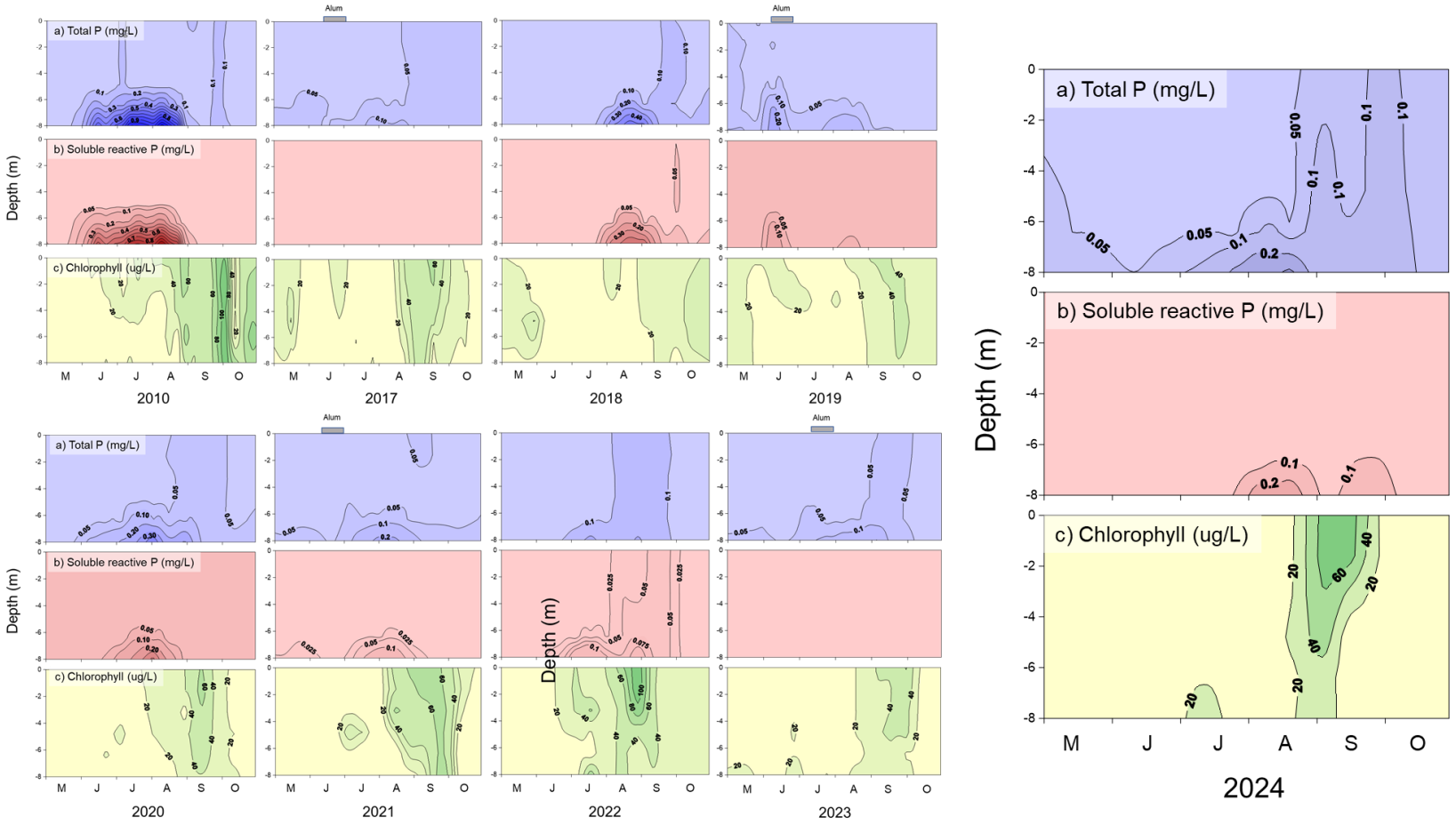

Figure 10. Seasonal and vertical variations in a) total phosphorus (P), b) soluble reactive P, and c) chlorophyll in 2010 (pretreatment) versus 2017-24 (post-treatment). Alum was applied in June 2017, 2019, 2021, and 2023.

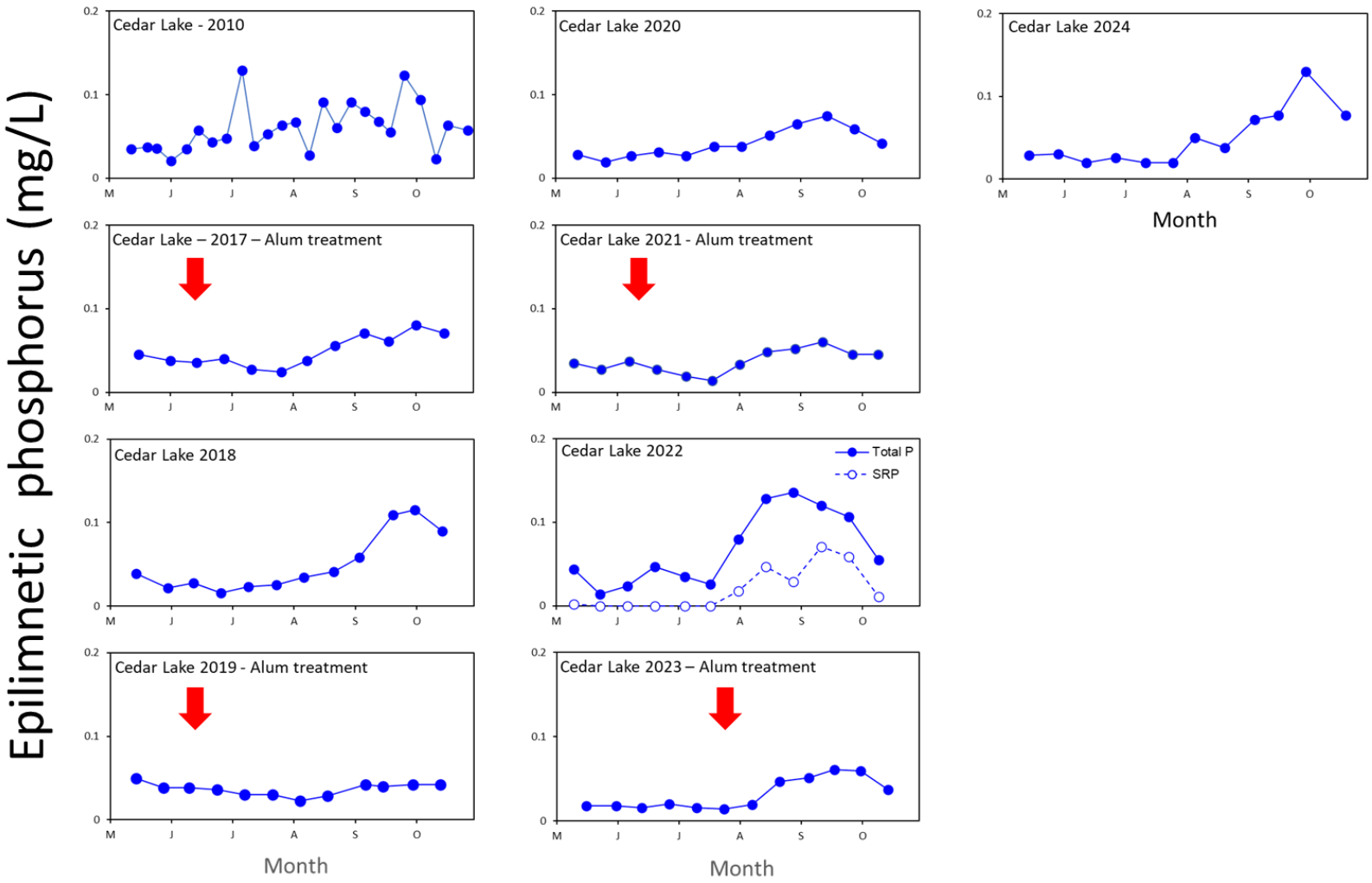

Figure 11. Seasonal variations in surface total phosphorus (P), during a pretreatment year (2010) and the post-alum treatment years 2017-24. Alum was applied in June 2017, 2019, 2021, and 2023.

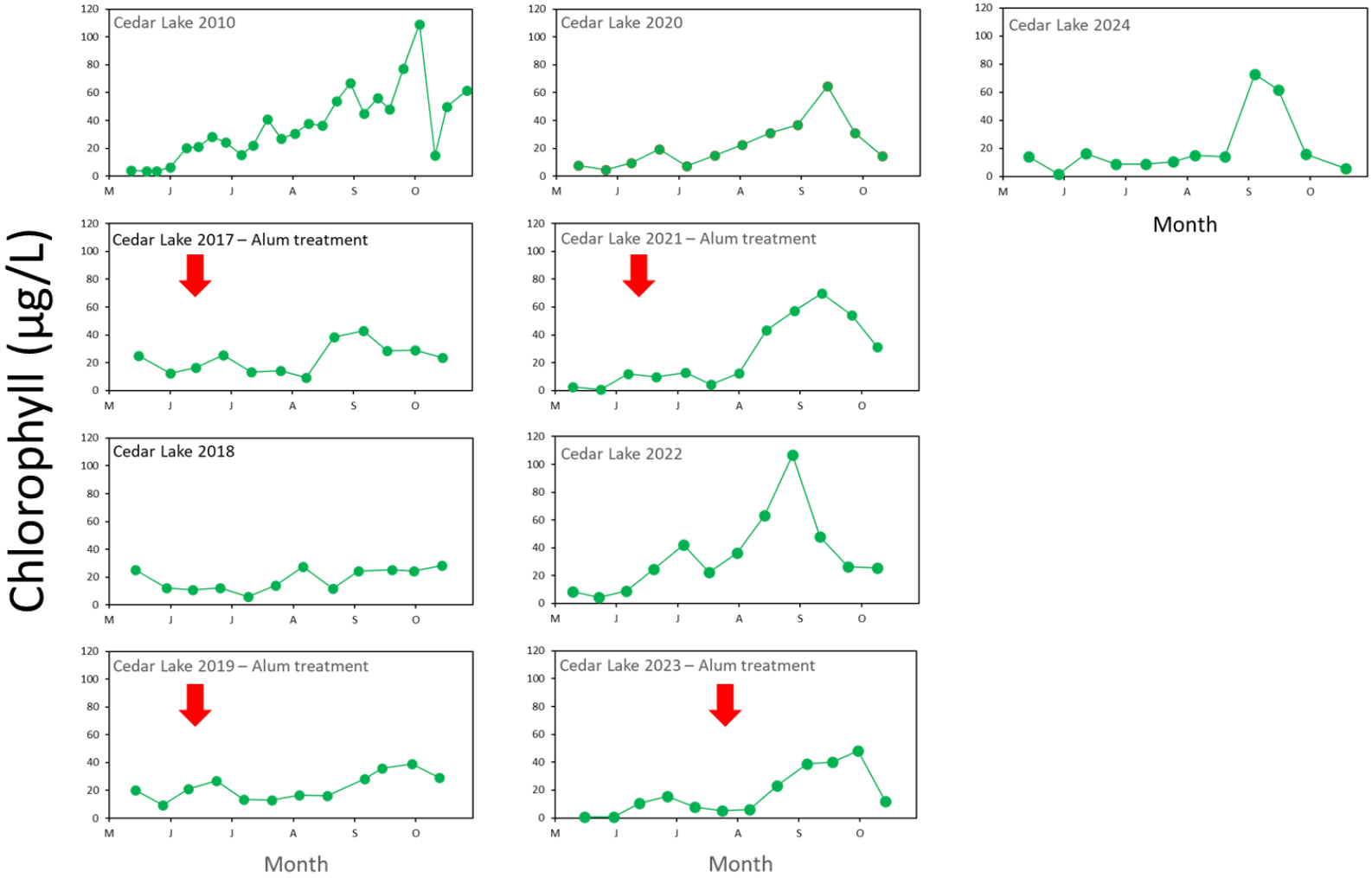

Figure 12. Seasonal variations in surface chlorophyll during a pretreatment year (2010) and the post-alum treatment years 2017-24. Alum was applied in June 2017, 2019, 2021, and 2023.

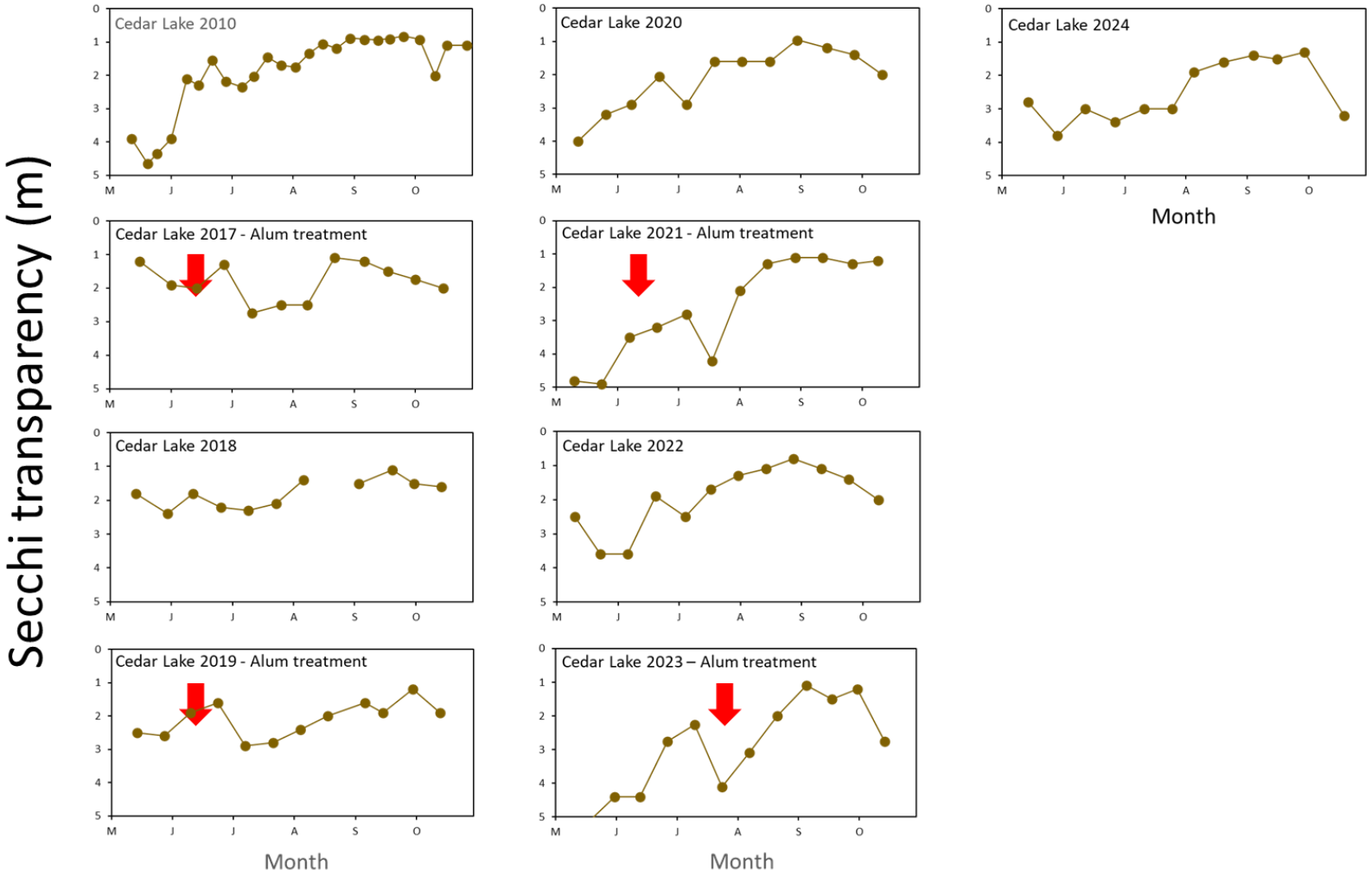

Figure 13. Seasonal variations in Secchi transparency during a pretreatment year (2010) and the post-alum treatment years 2017-24. Alum was applied in June 2017, 2019, 2021, and 2023.

Figure 14. Relationships between Secchi transparency and chlorophyll (upper panel) and total phosphorus (P) versus chlorophyll (lower panel) during the summer 2017-2024.

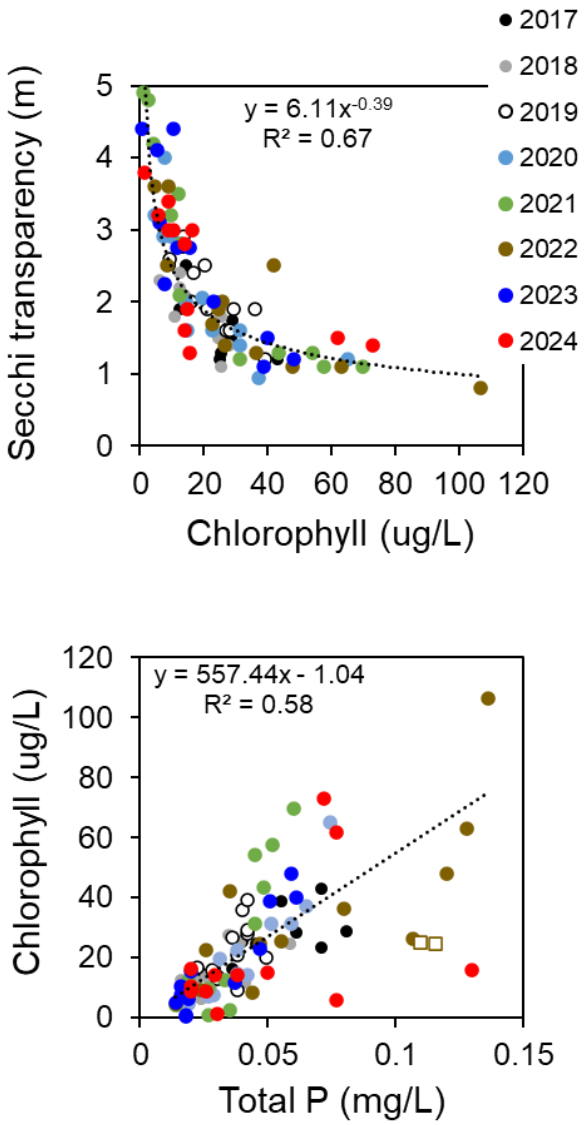

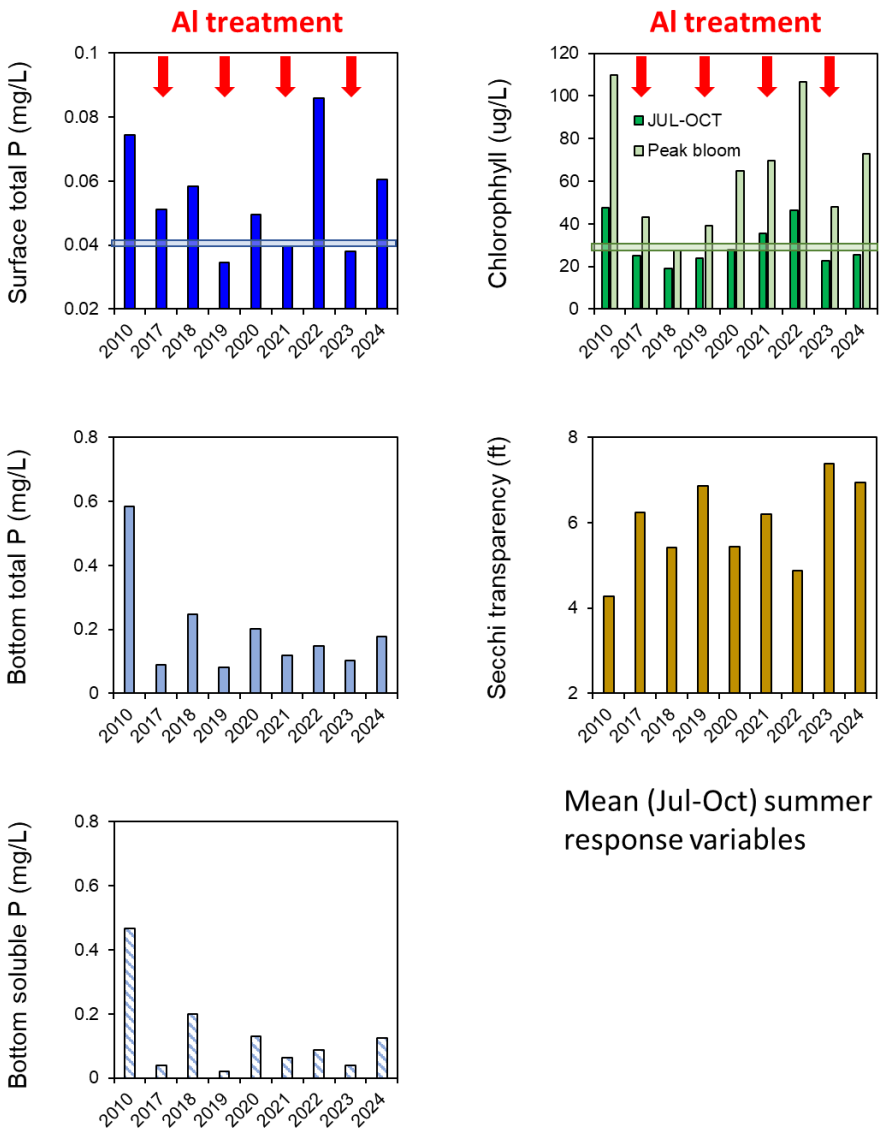

Figure 15. A comparison of mean summer (July-early October) summer concentrations of surface and bottom total phosphorus (P) and soluble reactive P (SRP), chlorophyll and Secchi transparency during a pretreatment year (2010) and the post-treatment years 2017-24. Alum was applied in June 2017, 2019, 2021, and 2023. Horizontal lines denote WisCALM target goals.

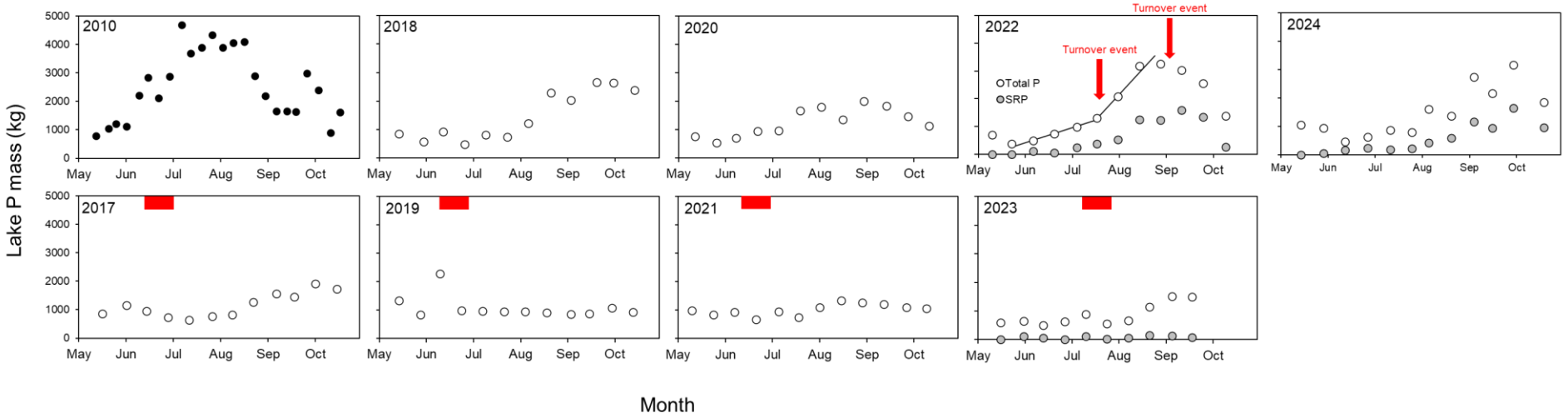

Figure 16. Seasonal variations in total phosphorus (P) mass during a pretreatment year (2010) and the post-treatment years 2017-24. Alum was applied in June 2017, 2019, 2021, and 2023.

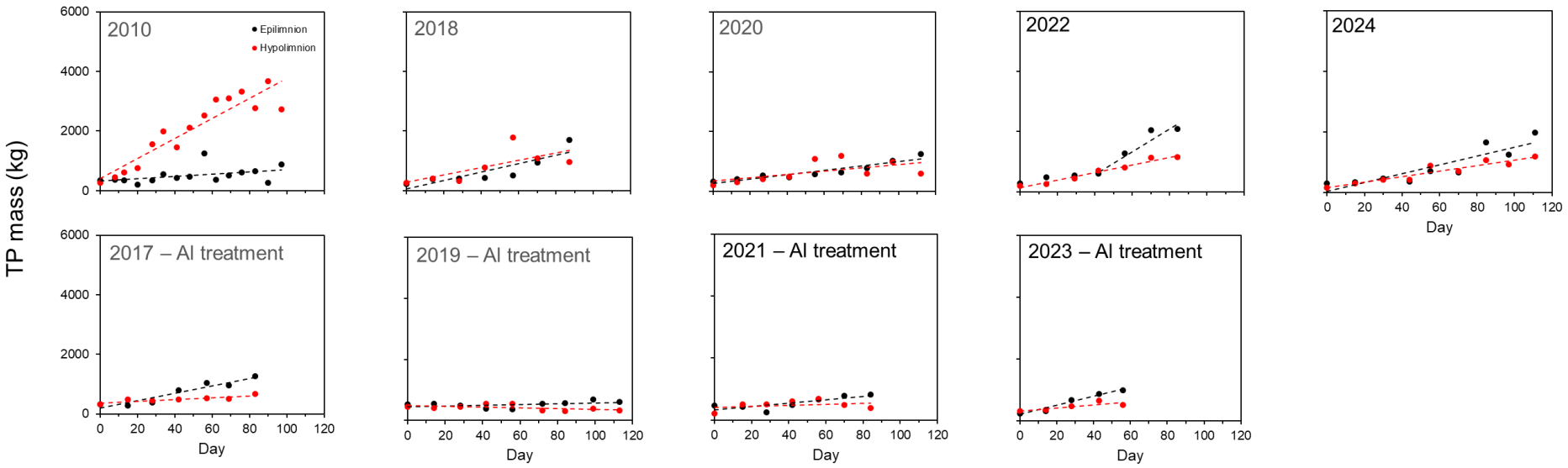

Figure 17. Seasonal variations in total phosphorus (P) mass in the epilimnion (i.e., 0-4 m) and hypolimnion (> 4 m) during a pretreatment year (2010) and the post-treatment years 2017-24. Alum was applied in June 2017, 2019, 2021, and 2023.

Figure 18. Variations in lake phosphorus (P) mass accumulation before (2010) and after 1st through 4th alum application.

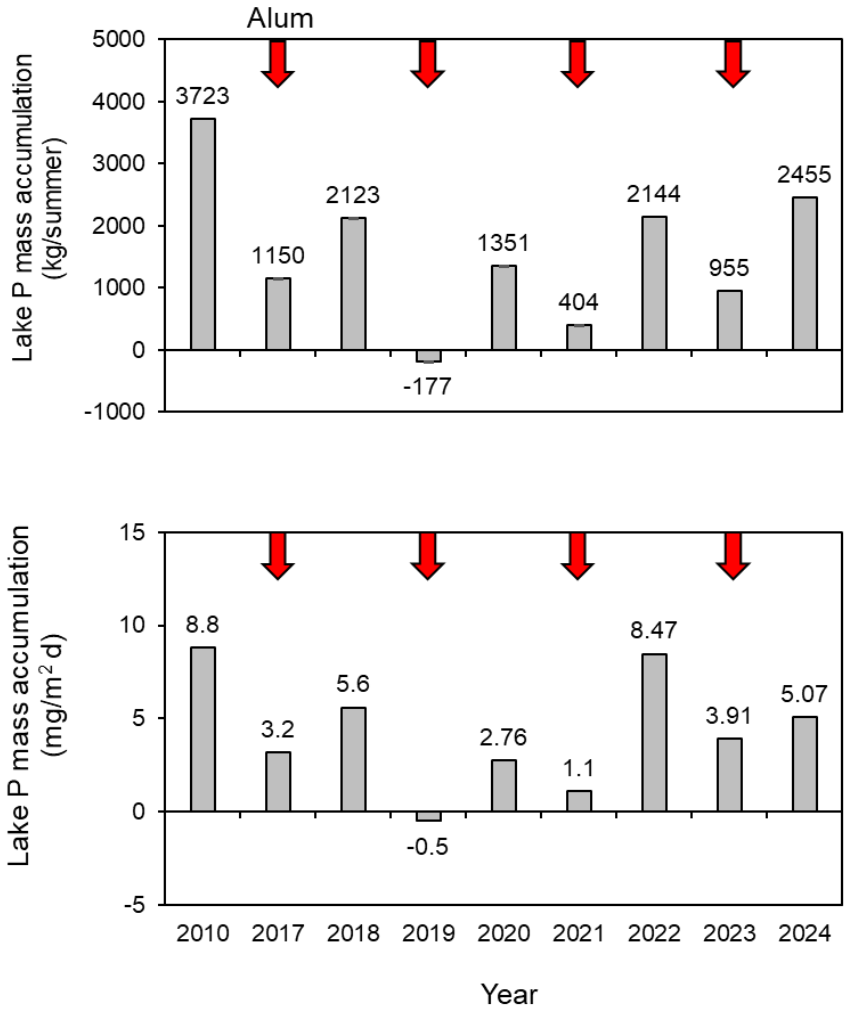

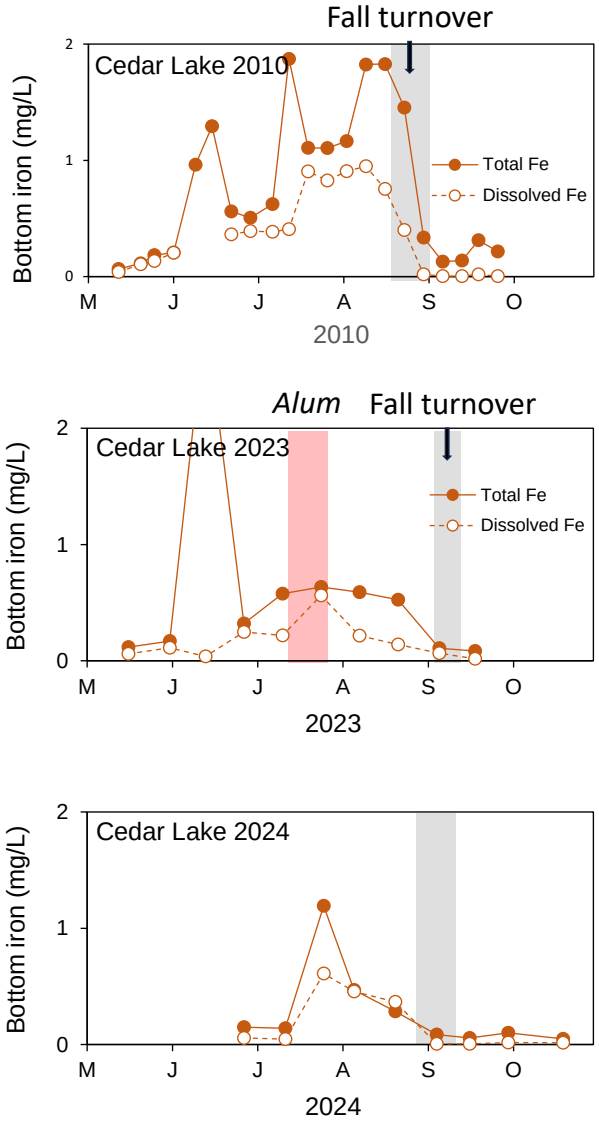

Figure 19. Variations in total and dissolved iron (Fe) at the lake bottom in 2010 (i.e., before Al applications) and 2023-24 (i.e., after the 4th Al application)

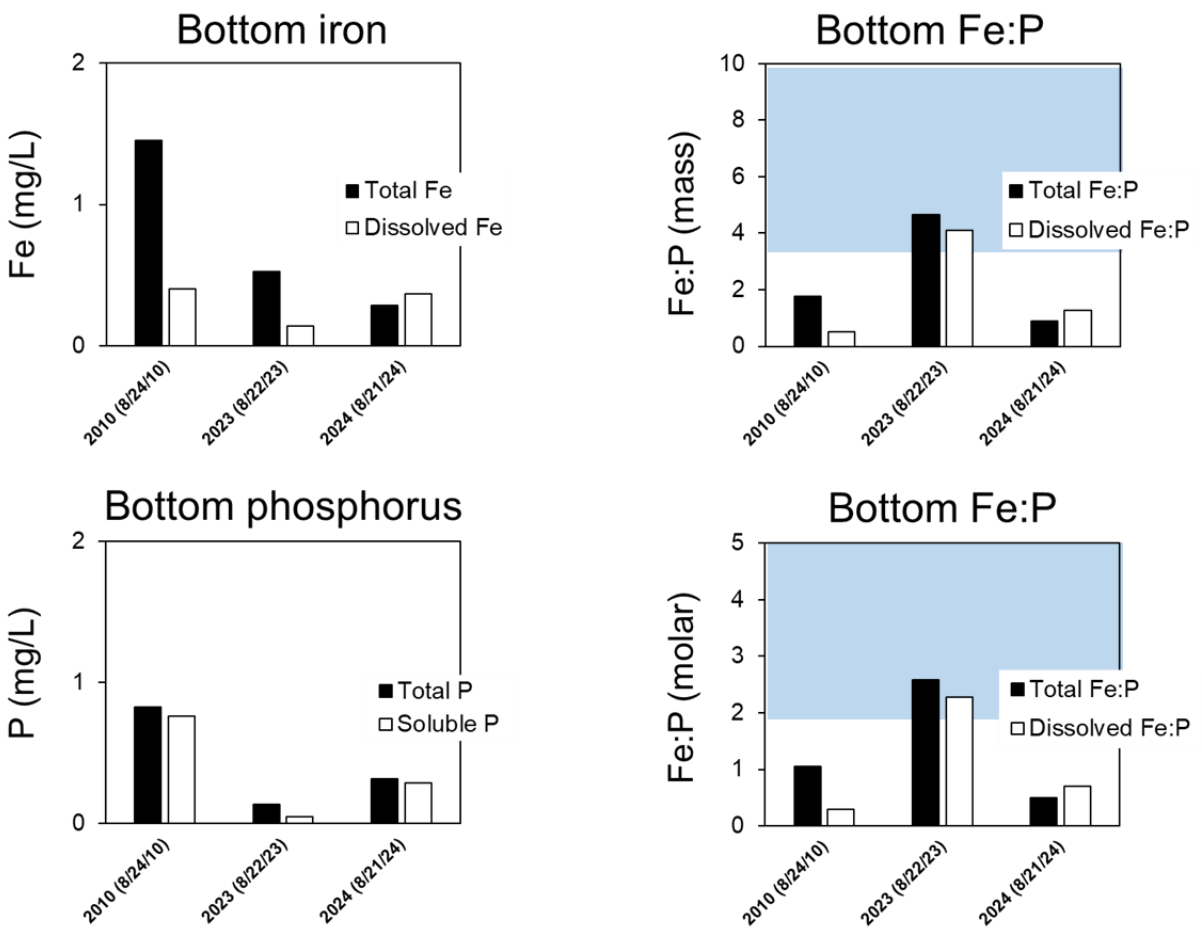

Figure 20. Variations in total and dissolved iron (Fe) and total and soluble phosphorus (P) at the lake bottom ~ 1 week prior to Fall turnover in 2010 (i.e., before Al applications) and 2023-24 (i.e., after the 4th Al application). Shaded areas denote the Fe:P ratio range needed to precipitate out all the soluble P during Fall overturn.

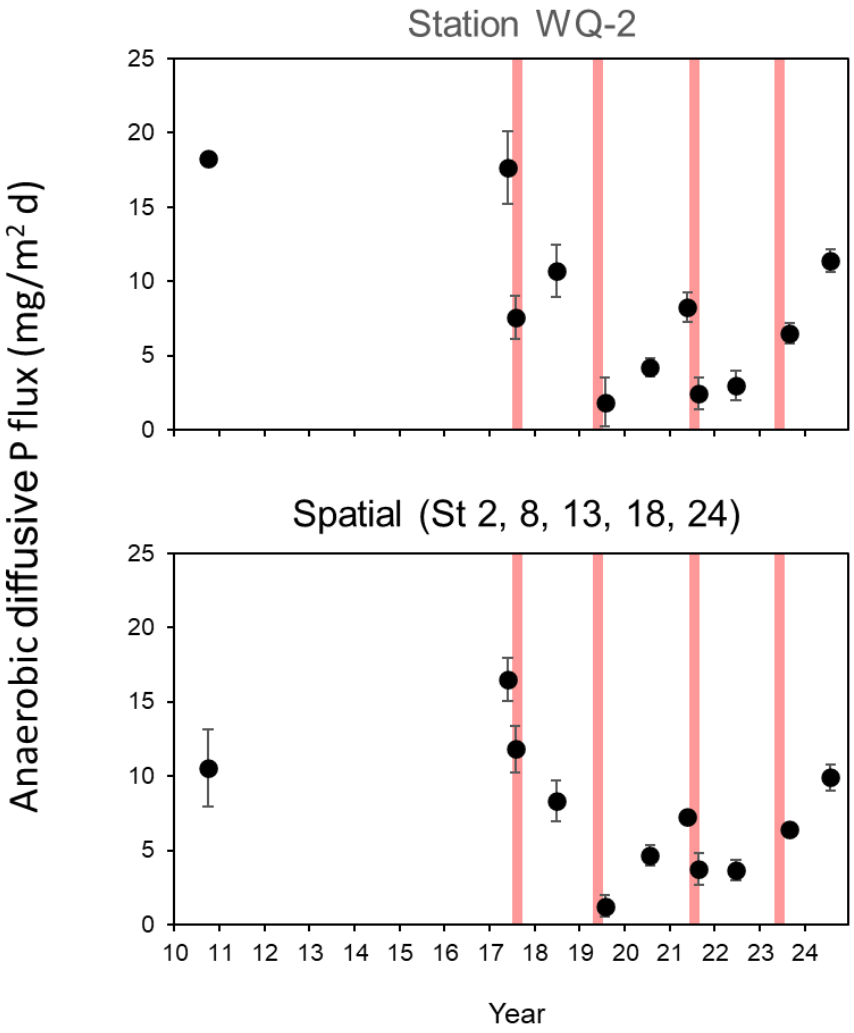

Figure 21. Variations in anaerobic diffusive phosphorus (P) flux (mg/m^2 d) before (June 2010 and 2017) and after the 1st through 4th alum application (horizontal red columns). WQ-2 = the centrally-located water quality sampling station. Spatial = the means from stations 3, 8, 13, 18, and 24 (see Fig. 1).

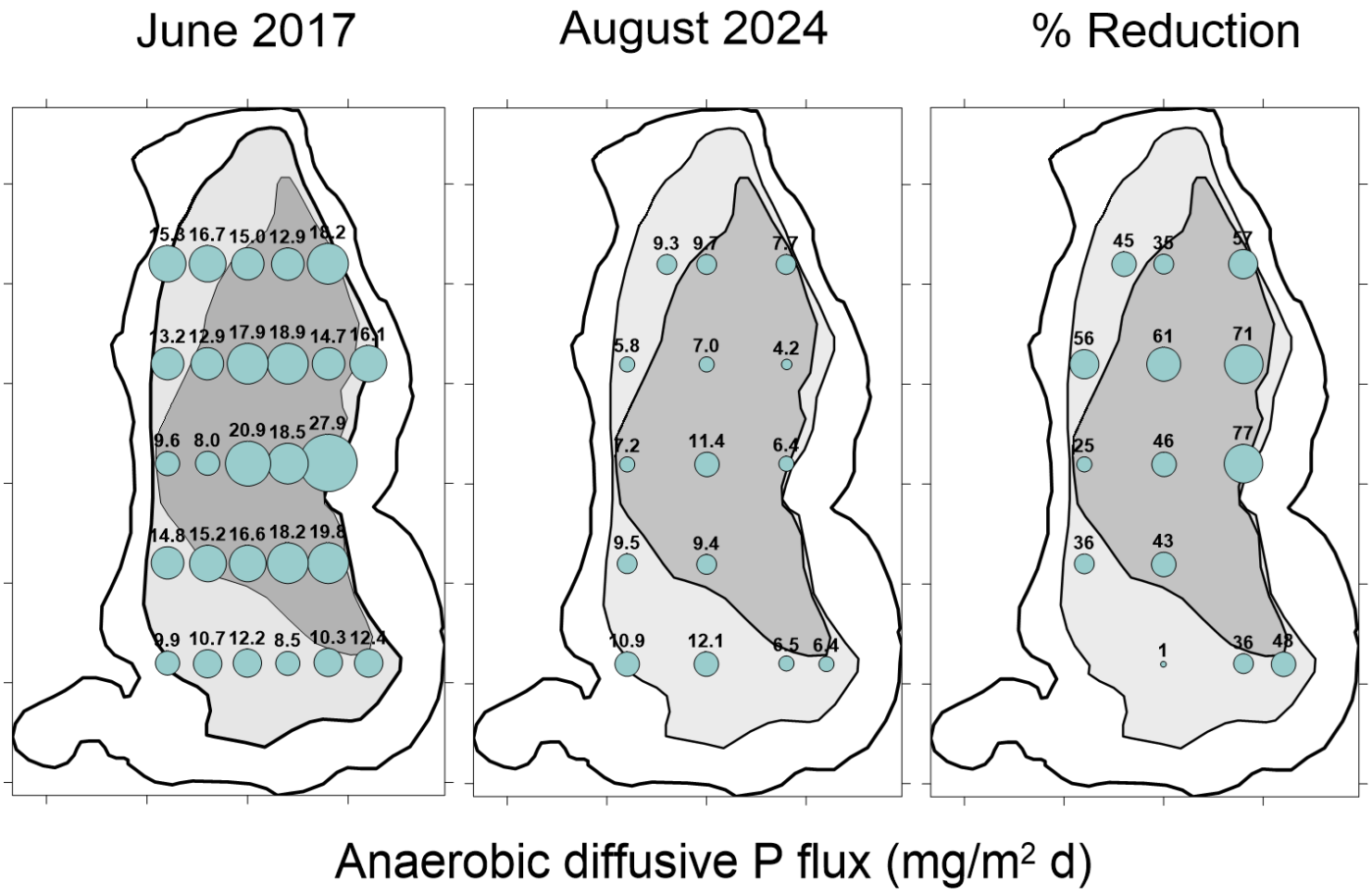

Figure 22. A comparison of spatial variations in laboratory-derived anaerobic diffusive P flux from sediment immediately before the initial alum treatment in 2017 (left), after the 4th alum application in 2023 (center), and percent improvement or reduction as of 2024 (right).

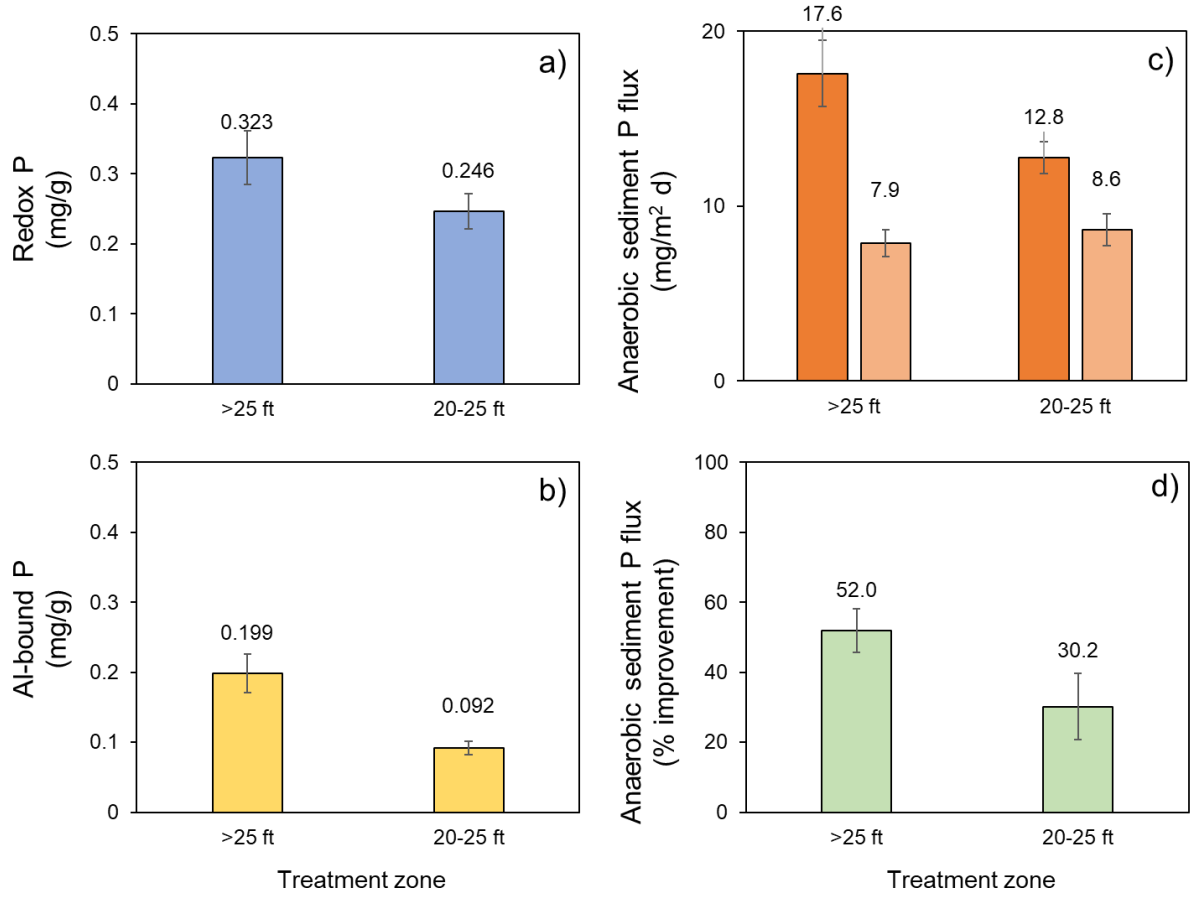

Figure 23. Mean redox P (a), aluminum-bound P (b), laboratory-derived anaerobic diffusive P flux (c), and anaerobic P flux percent improvement or reduction in 2024 (d) in the > 25-ft depth contour treatment zone (n=8) versus the 20-ft to 25-ft depth contour treatment zone (n=7).

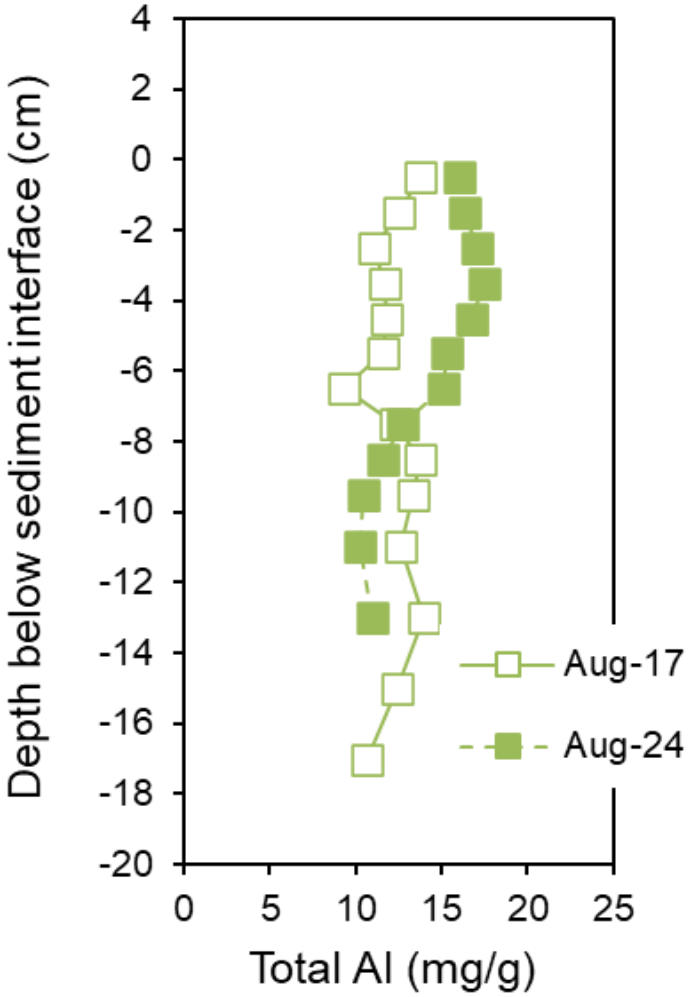

Figure 24. Vertical variations in total aluminum (Al) concentrations for a sediment core collected from station WQ2 in 2024 (Figure 1) The sediment profile represents post-alum treatment conditions after three alum applications (2017, 2019, 2021, and 2023). Green shaded area denotes the Al floc layer concentration increase since the first alum application in 2017.

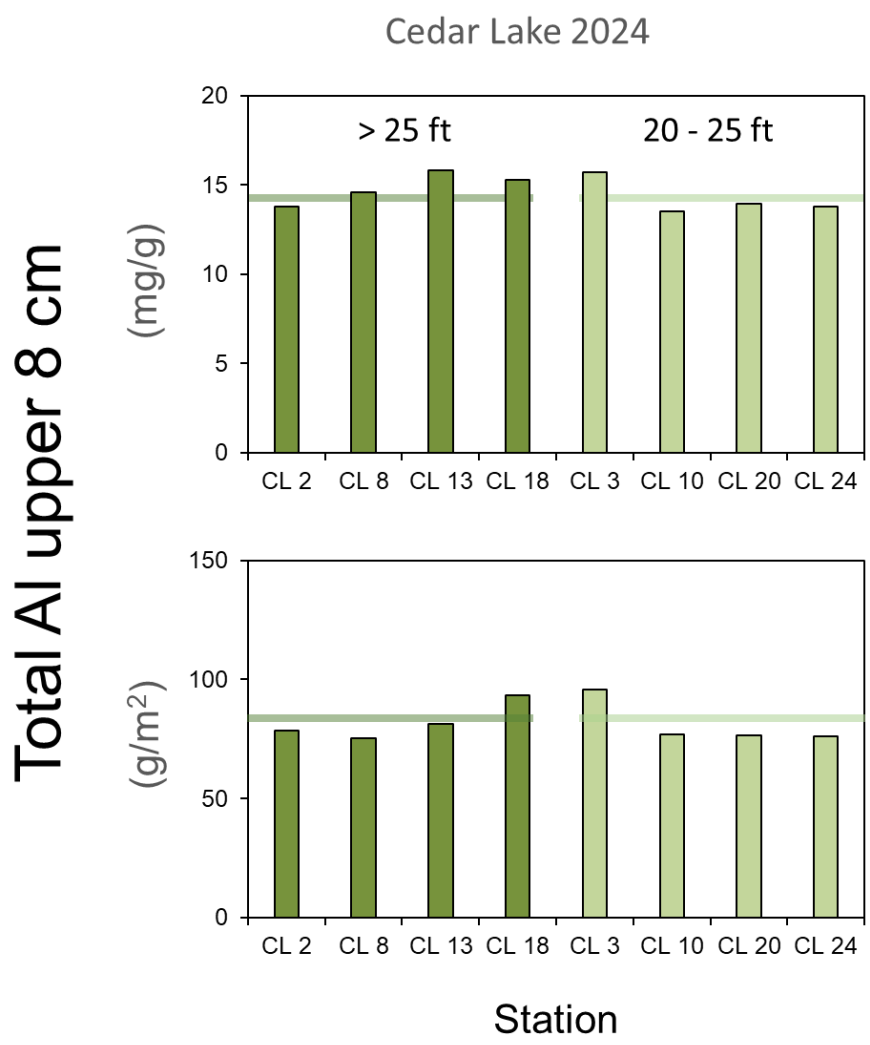

Figure 25. Total aluminum concentrations (mg/g upper panel, g/m^2 lower panel) in the upper 8-cm sediment layer at several stations located at > 25 ft, and a shallower station located between 20 ft and 25 ft. The > 25-ft depth contour was treated with a total of 121 g/m^2 while the 20-25-ft depth contour has been treated with a total of 68 g/m^2 alum since 2017. Horizontal lines represent the mean concentration within each depth stratum.

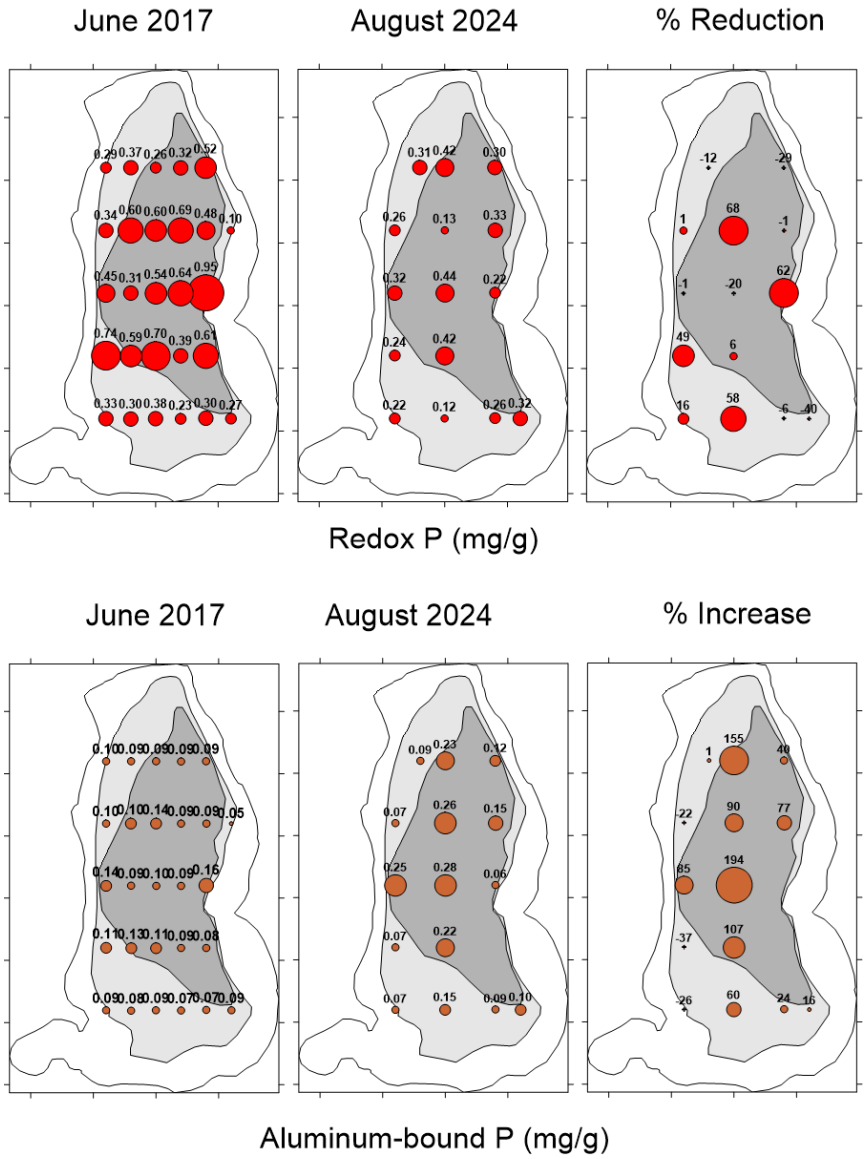

Figure 26. A comparison of spatial variations in surface sediment redox P (upper) and aluminum-bound P (lower) immediately before the initial alum treatment in 2017, after the 4th alum application in 2024.

Figure 27. Vertical variations redox P (i.e., the sum of the loosely-bound P and iron-bound P sediment fractions) and aluminum (Al)-bound P concentrations for a sediment core collected from station WQ2 (Figure 1) in June 2017 and August 2024. The sediment profile in June 2017 represents pre-treatment conditions while September 2023 represents post-alum treatment conditions after four alum applications (2017, 2019, 2021, and 2023).

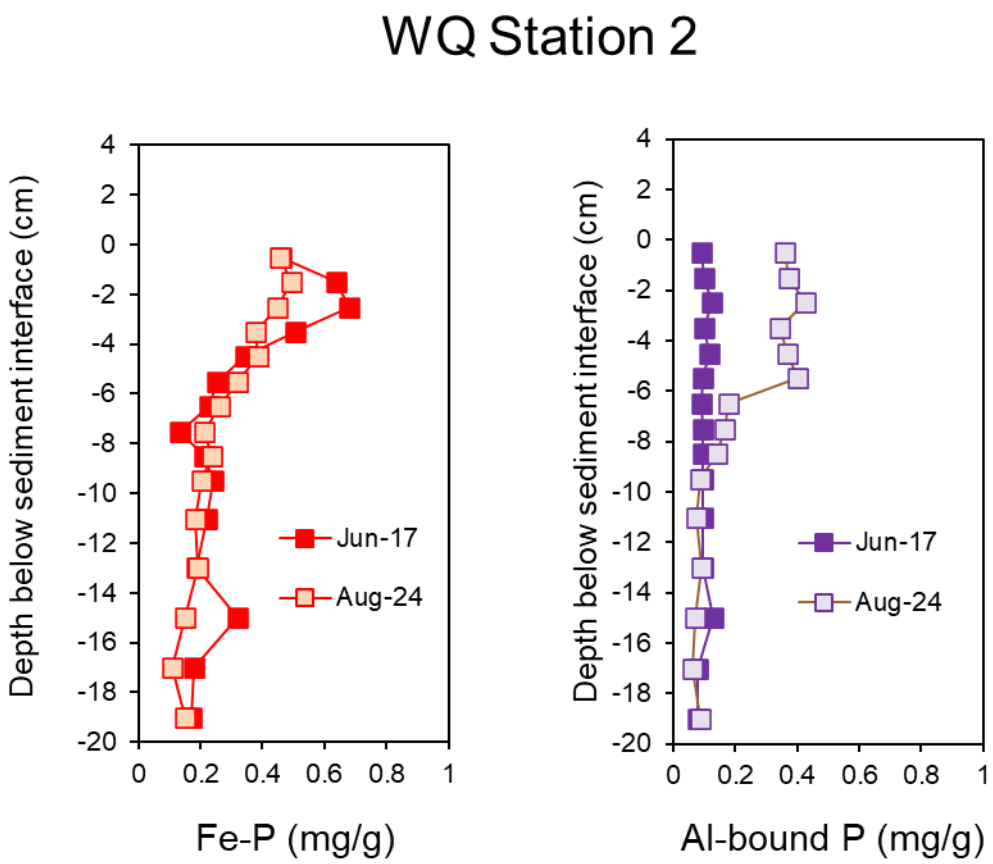

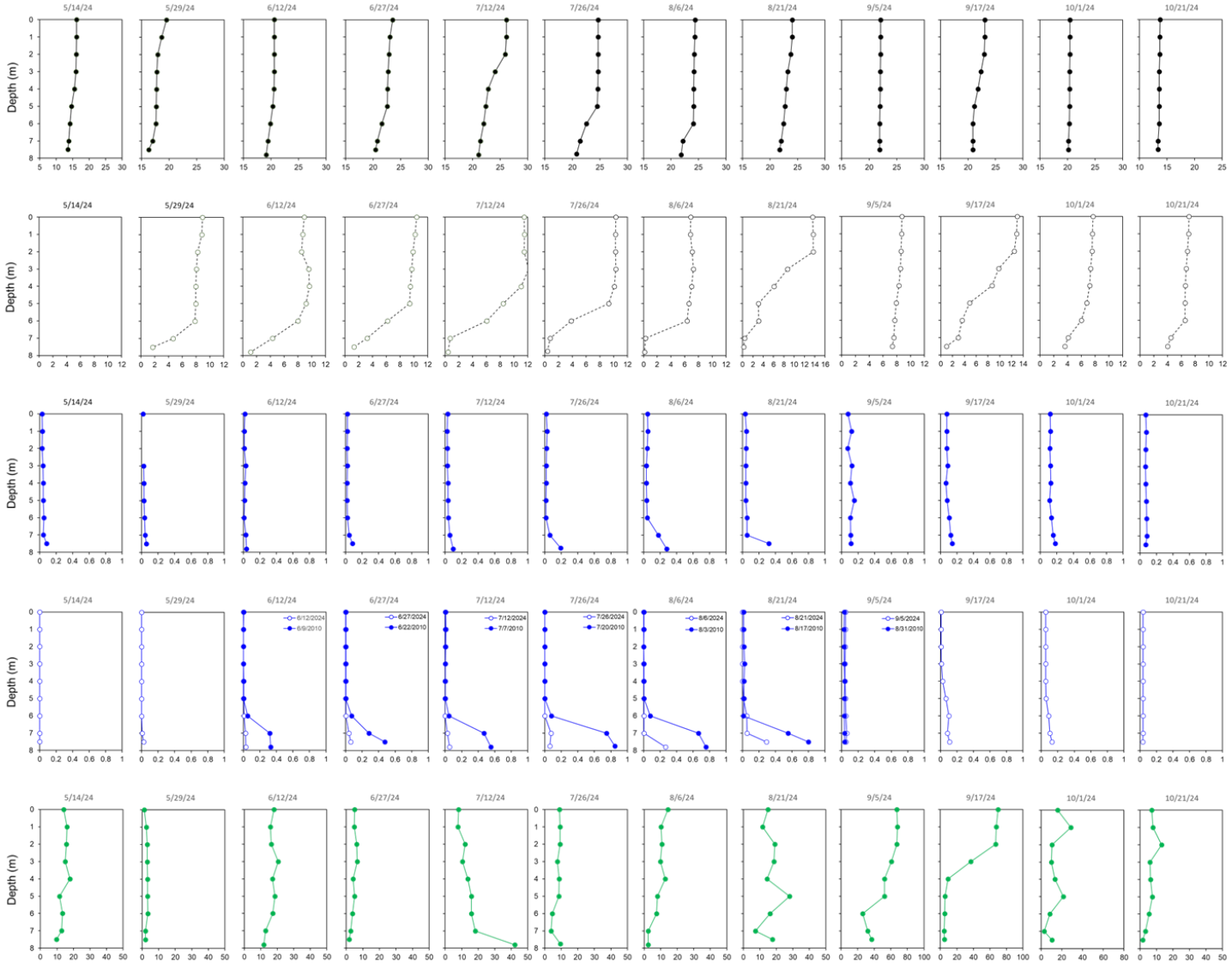

Appendix 1. Detailed vertical water column profiles of water temperature, dissolved oxygen, total P, soluble P, and chlorophyll for various dates in 2024.